# Dental morphology evolution in early peratheriines, including a new morphologically cryptic species and findings on the largest early Eocene European metatherian

Killian Gernelle, Marc Godinot, Bernard Marandat, Dominique Téodori, Sandrine Ladevèze, Rodolphe Tabuce

*Historical Biology*, 2024. With 8 figures (DOI: https://doi.org/10.1080/08912963.2024.2403602)

# Dental morphology evolution in early peratheriines, including a new morphologically cryptic species and findings on the largest early Eocene European metatherian

Killian Gernelle[a], Marc Godinot[b], Bernard Marandat[a], Dominique Téodori[c], Sandrine Ladevèze[d,e] and Rodolphe Tabuce[a,e]

[a] Institut des Sciences de l'Évolution de Montpellier (ISEM, UMR 5554), Univ Montpellier, CNRS, IRD, cc64, Place Eugène Bataillon, F-34095 Montpellier Cedex 05, France

[b] Ecole Pratique des Hautes Etudes, PSL, UMR 7207, CR2P, 8 rue Buffon, F75005, Paris, France

[c] 8 impasse de San Marino, 31140 Pechbonnieu, Haute-Garonne, France

[d] Centre de Recherche en Paléontologie - Paris (CR2P, UMR 7207), Sorbonne Université, Muséum National d'Histoire Naturelle, CNRS, 8 rue Buffon, F-75005, Paris, France

[e] Co-senior authors

CONTACT

Corresponding author: Killian Gernelle

Email address: killian.gernelle@umontpellier.fr

ORCID

Killian Gernelle: https://orcid.org/0000-0001-9698-0223

Sandrine Ladevèze https://orcid.org/0000-0001-6009-4107

Rodolphe Tabuce: https://orcid.org/0000-0002-4713-3981

**ABSTRACT** The initial stages of the evolutionary history of peratheriines, the European herpetotheriid metatherians, are largely unknown, primarily due to their limited morphological dental disparity throughout the Palaeogene, coupled with significant intraspecific variation. Based on eleven molars, we document a new early peratheriine species, ***Peratherium musivum* sp. nov.**, which is larger than and morphologically similar to the earliest peratheriine, *Peratherium constans* (MP7). Subtle molar characters are shared with the largest early Eocene peratheriine, ***Peratherium maximum* comb. nov.** We illustrate the importance of studying possible changes in molar cusp - basin proportions and correlated characters that occured during peratheriine evolution. *Peratherium musivum* sp. nov., which spanned only part of the MP7-MP8+9 time interval, and the ~MP8+9 *Peratherium maximum* comb. nov., were probably widespread in Western Europe. The description of a well-preserved mandible of the latter, from La Borie (~MP8+9), reveals original features concerning relative size and shape of dental alveoli, partly corroborated using isolated molars. These traits are absent in the younger, most representative species of both peratheriine genera, *Peratherium* and *Amphiperatherium*. Based on the aforementioned data and a critical review, it is demonstrated that peratheriine genera lack consistent definitions, so that the *Peratherium*/*Amphiperatherium* dichotomy is plausibly inapplicable to early Eocene representatives.

**KEYWORDS** France, Herpetotheriidae, Marsupialiformes, molars, systematics, Ypresian.

This article is registered in ZooBank under urn:lsid:zoobank.org:pub:A2B4DE58-855C-4CB8-BC1D-C9677E6DF97D

## Introduction

Herpetotheriidae are a possibly paraphyletic (with respect to crown-marsupials) assemblage of extinct and small (much less than 500 g) Cenozoic stem-marsupials, with a superficially 'opossum-like' unspecialised tribosphenic dentition (e.g., Sanchez-Villagra et al. 2007; Ladevèze et al. 2020; Beck 2023). The subfamily Peratheriinae, almost restricted to Europe, with one species documented in Africa (Simons and Bown 1984; Hooker et al. 2008; Crespo and Goin 2021), includes the genera *Peratherium* Aymard, 1850, and *Amphiperatherium* Filhol, 1879, while North American herpetotheriids, Herpetotheriinae, are assumed to be represented by *Herpetotherium* Cope, 1873, during the early Eocene (Korth 1994, 2008; Williamson et al. 2012; Ladevèze et al. 2020). The origin of unequivocal herpetotheriids (i.e., Eocene to Miocene representatives) is uncertain (e.g., Johanson 1996; Martin et al. 2005; Ladevèze et al. 2012; Williamson et al. 2012); so are their precise intrafamilial relationships (Figure 1), largely because of difficulties in establishing the polarity of labile, often homoplastic and only dental characters (Szalay 1993, p. 220). However, characterising the morphology of the earliest representatives of a given family is crucial in order to understand possible ancient intrafamilial cladogenesis (e.g., Marivaux et al. 2004, p. 108).

The oldest peratheriine, and oldest species of the genus *Peratherium*, is the small *Peratherium constans* Teilhard de Chardin, 1927, from the earliest Eocene of Dormaal (Belgium, MP7 reference level, usually correlated with the Paleocene-Eocene Thermal Maximum [PETM]; Steurbaut et al. 2003; Ladevèze et al. 2012) (Figure 1). The distinction of earliest representatives of *Peratherium* and *Amphiperatherium* is challenging (Hooker et al. 2008, p. 643). In fact, *Amphiperatherium brabantense*, Crochet, 1979, also defined in Dormaal (Crochet 1979), has been considered a junior synonym of *Peratherium constans* (Ladevèze et al. 2012). As a consequence, *Amphiperatherium maximum* Crochet, 1979, typical of the MP8+9 and ~MP8+9 faunas of the Paris Basin (Crochet 1980, p. 98-99), and also reported in localities older than MP8+9 (e.g., Russell et al. 1988), becomes one of the earliest species of the genus *Amphiperatherium* (Figure 1), and the only species of *Amphiperatherium* with its type locality in the early Eocene (Crochet 1979; Ladevèze et al. 2012), which implies an ancient divergence between *Peratherium* and *Amphiperatherium*. *Amphiperatherium maximum* and closely related taxa (e.g., *Amphiperatherium* aff. *maximum*; Storch and Haubold 1989) are also the largest metatherians of the early to middle Eocene of Europe (Figure 1). This species possibly initiates the species rich 'lineage' (*sensu* Crochet 1980) of relatively large peratheriines *A. maximum* – *A. bastbergense* Crochet, 1979 – *A. fontense*

Crochet, 1979 (Figure 1) – *A. ambiguum* (Filhol, 1877), which persists until the early Oligocene, according to Crochet (1980: fig. 151).

The taxonomy and intrasubfamilial relationships of peratheriines remain particularly unclear between the MP7 and MP8+9 reference levels, which is the time interval encompassing the first steps of their evolutionary history, after their appearance in the fossil record (Figure 1). In fact, the temporal resolution of the Ypresian MP reference levels (see BiochroM'97 1997) appears insufficient to describe metatherian evolution, as (i) the range of some species is solely restricted between two reference levels (Gernelle et al. 2024), and (ii) the ages of various southwestern MP7-MP8+9 interval localities (i.e., in the time range between MP7 and MP8+9, excluding MP7 and MP8+9/~MP8+9 localities), as deduced from recent bio- and chemostratigraphic analyses, are more accurately estimated, notably relative to the Eocene Thermal Events (ETMs; Yans et al. 2014; Noiret et al. 2016). Furthermore, since the taxonomic revision of Crochet (1980), rare molars from the French localities of the MP7-MP8+9 time interval have been allocated to *Amhiperatherium* cf. *maximum* (Godinot 1981; Marandat 1991; Louis 1996), vaguely denoting molars smaller than those of *A. maximum*, but larger than those of small early peratheriines such as *Peratherium constans* (Figure 1).

In this study, based on both ancient and unpublished dental material, we describe a new morphologically cryptic peratheriine species that is intermediate in size between *Peratherium constans* and '*Amphiperatherium*' *maximum* (the taxonomic status of the latter being discussed). This represents the first new peratheriine species to be described since *Peratherium africanum* Simons & Bown, 1984, and is the second oldest early Eocene peratheriine. Secondly, a detailed description of a new mandible of *Peratherium maximum* comb. nov., the most complete specimen known and the first record of this species in southwestern France, compared to (i) the type serie of the species, and (ii) younger peratheriines, is used as a basis in order to thoroughly discuss the problematic generic taxonomy of Peratheriinae. Throughout this work, we also highlight and discuss several dental characters, some of them being correlated, assumed to bear a phylogentic signal in early peratheriines, which is an essential first step towards resolving the complex systematics of this subfamily (Figure 1).

**Institutional and locality abbreviations**

AMNH, American Museum of Natural History, New York; IRSNB-M, mammal collection of the Royal Belgium Institute of Natural Sciences; MNHN.F., fossil collection of the Muséum

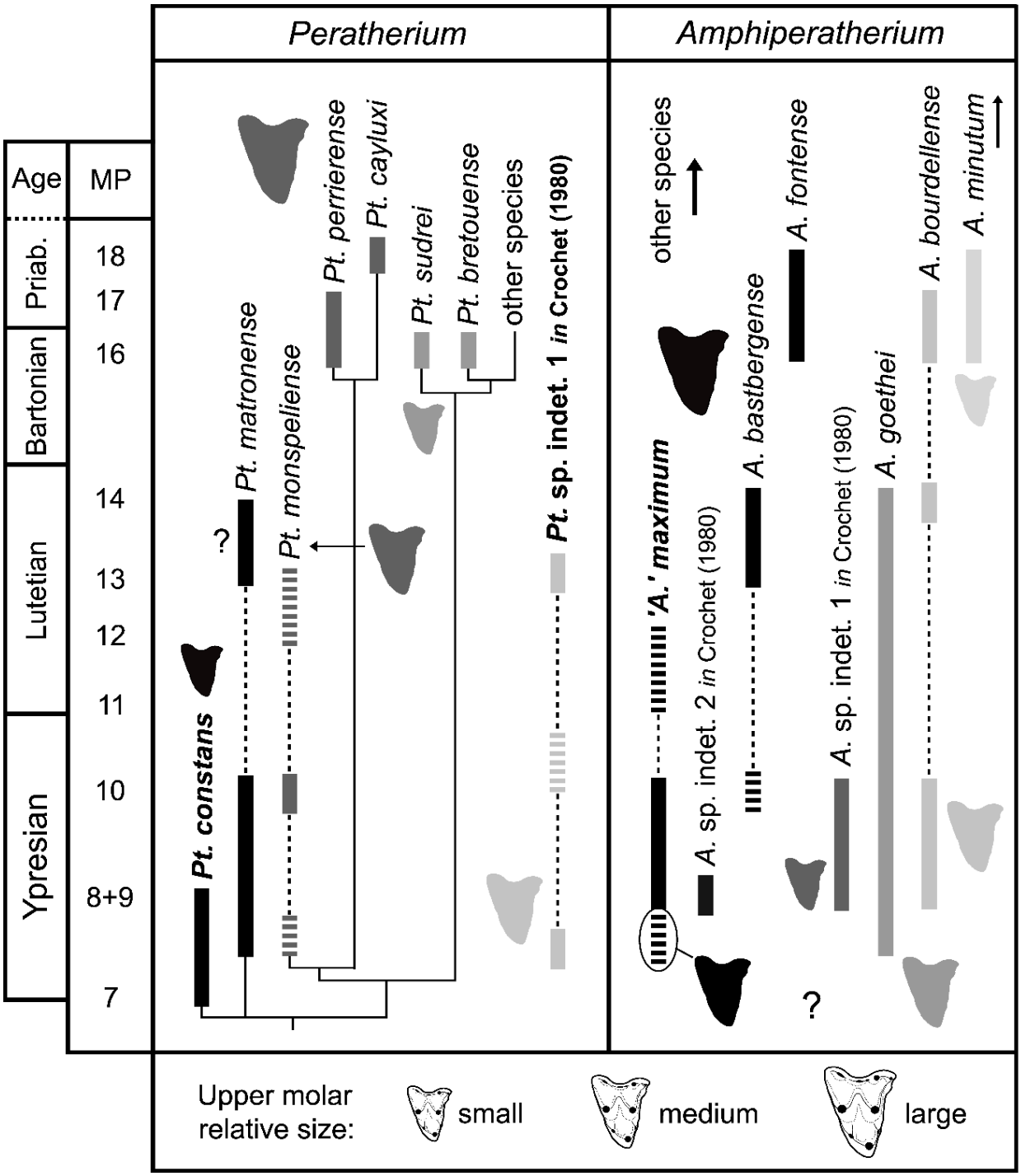


**Figure 1.** Approximate temporal extensions of most European *Peratherium* – *Amphiperatherium* species during the Eocene (Ypresian to early Priabonian; MP7 to MP18 reference levels, BiochroM'97 1997), as conceived before this work. Within both genera, species plotted with different colours have been allocated to different lineages *sensu* Crochet (1980). All 'lineages' which have been assumed to emerge during the early Eocene are represented. Names in bold indicate the most studied Ypresian species in this work. Dashed temporal extensions indicate occurrences in open nomenclature. Relative sizes, represented by upper molar outlines, follow specific diagnoses of Crochet (1980). Partial hypothetical relationships of *Peratherium* species as proposed by Hooker et al. (2008) are depicted.

?*Peratherium giselense* Heller, 1936, is not included, because its generic status has been disputed (see Kurz 2007). The relative positioning of MP reference levels and Eocene ages follow Speijer et al. (2020). The 'MP15' is not figured, because the Bartonian age of the reference locality of La Livinière 2 has been challenged (e.g., Luccisano et al. 2020). Occurrence data are from Crochet (1980), Godinot (1981), Dégremont et al. (1985), Marandat (1986), Peláez-Campomanes et al. (1989), Storch and Haubold (1989), Sudre et al. (1990), Marandat (1991), Legendre et al. (1992), Kurz (2007), Ladevèze et al. (2012), and Vianey Liaud et al. (2024). Abbreviation: Priab., Priabonian.

National d'Histoire Naturelle, Paris; MNHN.F.AV, Avenay; MNHN.F.CB, Condé-en-Brie; MNHN.F.ME, Meudon; MNHN.F.PY, Pourcy; MNHN.F.RI, Rians; MNHN.F.SN, Soissons; NHMUK.PV.M, palaeontological vertebrate collection of the Natural History Museum, UK, London; NMB Om., Dormaal, collection of the Natural History Museum of Basel; UM-, palaeontological collection of the University of Montpellier; UM-AZI, Azillanet; UM-BOUX, Bouxwiller; UM-BRI, La Borie; UM-CLO, Le Clot; UM-FNR, Fournes; UM-SNB, Sainte-Néboule; UM-VBO, Valbro; UM-VIE, Vielase; USNM, United States National Museum.

**Other abbreviations**

Dental loci: MX, Xth upper molar; mX, Xth lower molar; pX, Xth lower premolar. Reference levels, biozones and hyperthermals: ETM2, Eocene Thermal Maximum 2; MP, Mammal Palaeogene reference level (BiochroM'97 1997); PE, Paleocene-Eocene biozone (Hooker 1996a); PETM, Paleocene-Eocene Thermal Maximum.

Measurements and descriptive statistics: L, maximal mesiodistal length; OR, observed range; pL, protocone length; pW, protocone width; S, approximate surface; sL, stylar shelf length; tL, talon length; tlW, talonid width; tlWr, relative talonid width; trW, trigonid width; tW, talon width; W, maximal labiolingual width.

## Ages of the localities

The here studied localities of Soissons (in Aisne) and Pourcy (in Marne) in northern France, of Le Clot (in Corbières), Fournes (in Minervois) and Rians (in Provence) in southern France, and of Abbey Wood (in London), are all considered in the time interval between MP7 and ~MP8+9 reference levels (Figure 2). Soissons and Le Clot are the oldest of these localities, and are, respectively, placed within and correlated with biozone PE II (Hooker 1996a; Marandat et al. 2012). While the precise age of Soissons is uncertain, Le Clot is positioned by bio- and chemostratigraphic analyses before the ETM2, approximately 1 myr younger than

the MP7 reference locality of Dormaal (~56 Ma), hence close to 55 Ma (Yans et al. 2014). Fournes is positioned by marine correlation and chemostratigraphic analysis just after the ETM2 (~54 Ma), closer in time to the MP8+9 than to the MP7 reference level (Noiret et al. 2016: fig. 2). Rians is a locality possibly similar in age to Fournes, based on mammalian biostratigraphy (Marandat et. 2012; Noiret et al. 2016; Philip et al. 2017, p. 328). The age retained for Abbey Wood (biozone PE III of Hooker 1996a) is 55.12 Ma (Hooker 2010), therefore older than Fournes and Rians. These last two thus necessarily correlate with biozone PE III instead of biozone PE II. The precise biochronologic age of Pourcy, ascribed to biozone PE III (Hooker 1996a), remains more controversial (Louis and Michaux 1962); this locality has been alternatively considered closer to MP7 or to MP8+9 reference levels (as summarised in Hand et al. [2015, p. 2] and Spijkerman et al. [2015, p. 176]), and relative biochronologic positioning with respect to Fournes, Rians, and Abbey Wood is lacking.

Biochronologic arguments position La Borie (in Lauragais, near the Saint-Papoul village; Laurent et al. 2010: fig. 1) close to the MP8+9 reference level (~MP8+9; Laurent et al. 2010). The mammal fauna of Condé-en-Brie (in the Paris Basin) is classically considered close in age to the mammal fauna of Avenay, which is the reference locality of the MP8+9 (Louis 1966; BiochroM'97 1997).

## Materials and methods

### Provenance of the specimens

The specimens from Soissons, Meudon (in Île-de-France; one specimen discussed), Rians, Pourcy, Avenay (two specimens used for comparisons), and Condé-en-Brie are housed in the palaeontological collections of the Muséum National d'Histoire Naturelle (MNHN.F.; Paris, France). The specimens from Le Clot, Fournes, La Borie, Bouxwiller (northeastern France; one specimen used for comparisons), Vielase (in Quercy phosphorites; one specimen used for comparisons), Sainte-Néboule (in Quercy phosphorites), and Valbro (in Quercy phosphorites) are housed at the University of Montpellier (UM-; southern France). The peratheriine hemi-mandible from La Borie (UM-BRI-17), described and figured in the present study, was found and prepared by one of us (DT). The single specimen from Abbey Wood is housed at the Natural History Museum, London (NHMUK.PV.M; England), and was studied via the photograph and measurements available in the literature (Hooker 2010). Casts of

herpetotheriine specimens (AMNH, USNM) housed at the University of Montpellier were used for comparisons with

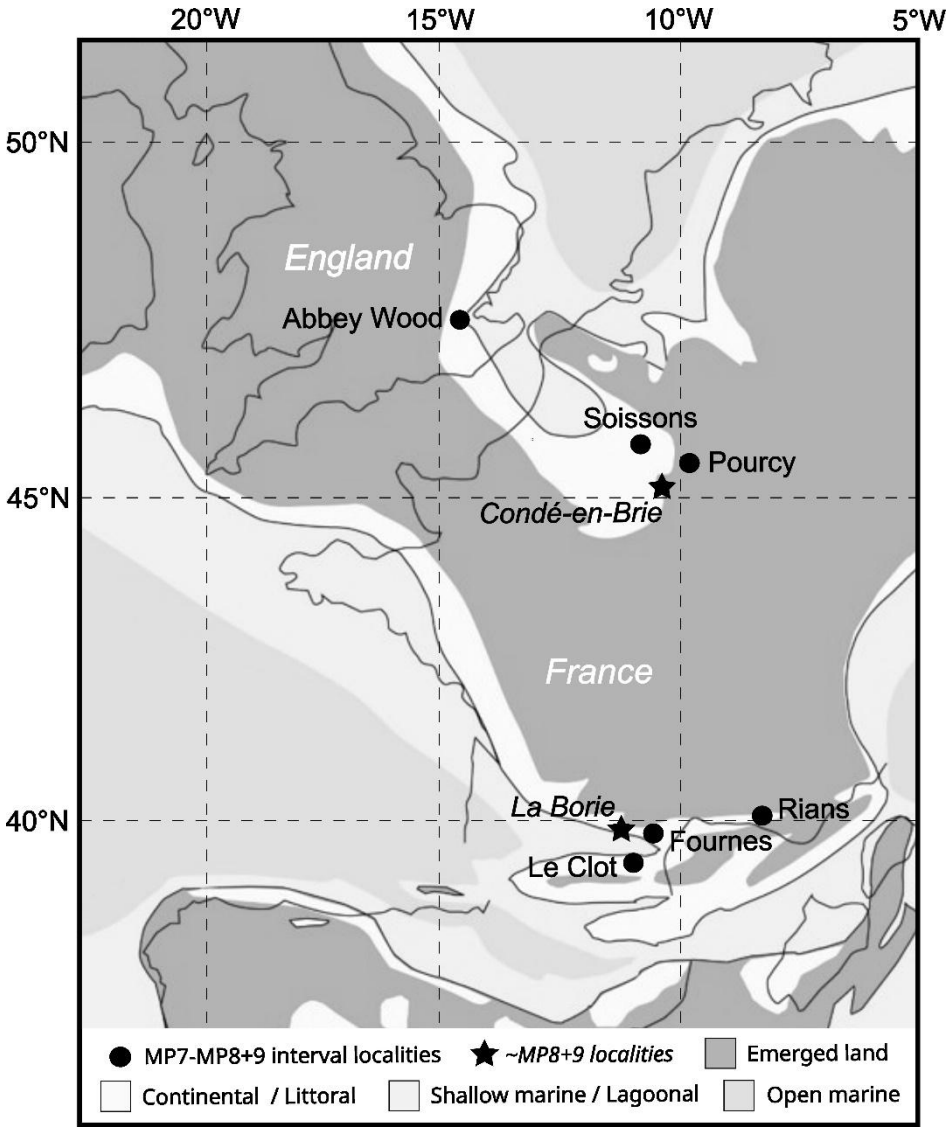


**Figure 2.** Paleogeographic map of France and England during the early Eocene (modified from Marandat et al. 2012) with the position of MP7-MP8+9 interval and ~MP8+9 localities studied.

peratheriines. Comparisons and measurements of molars of *Peratherium constans* from Dormaal have been made based on available illustrations from Ladevèze et al. (2012) (seven upper molars measured), and on casts from the University of Montpellier (seven upper molars measured), of which the original specimens are housed in the Royal Belgian Institute of Natural Sciences (IRSNB-M-; Brussels), and in the Natural History Museum of Basel (NMB; Costeur and Schneider 2011).

**High-resolution x-ray microtomography**

Illustrated specimens were scanned using a µ-CT-scanning station EasyTom 150 / Rx Solutions (Montpellier RIO Imaging, ISEM, Montpellier, France) by one of us (KG). Images

of these specimens were achieved using the 'snapshot' tool of Avizo® 9.3. Isolated molars were scanned with a resolution between 5.95 µm and 9.09 µm, depending on the specimen. All illustrations of isolated molars are based on volume renderings of the specimens. The hemi-mandible from La Borie (UM-BRI-17) was scanned with a resolution of 8.91 µm. The dentaries of the specimens UM-SNB-508 and UM-VBO-128, respectively scanned with a resolution of 9.96 µm and 8.00 µm, were isolated from cheek teeth by segmentation, in order to compare the morphology of their alveoli to those of UM-BRI-17. Volume rendering pictures of the complete UM-SNB-508 and UM-VBO-128 specimens, with the preserved lower cheek teeth, are also available in this study. For each of the three hemi-mandibles, a pre-segmentation of one slice every ~5-10 slices was performed, employing the 'lasso', 'magic wand' and 'blow' selection tools of Avizo® 9.3. The smart interpolation tool of the online platform Biomedisa (Lösel et al. 2020) was used to complete each segmentation.

**Dental anatomy and measurements**

The updated tribosphenic molar nomenclature illustrated in Gernelle et al. (2024: fig. 2) was adopted. Orientation and measurement methods of maximum length and width of tribosphenic upper and lower molars also follow Gernelle et al. (2024: fig. 2); i.e., the paracone – metacone axis of upper molars and the paraconid – metaconid axis of lower molars were used as reference (see Clemens [1966, p. 4] for lower premolars). Mandibular heights were taken on the lingual aspect of the mandible, from its ventral edge to the adjacent dorsal molar alveolus. All measurements are given with an accuracy of 0.01 millimetres. All measurements were made on screenshots of volume rendering or surface models of the scanned specimens (see below), using Avizo® 9.3 (Thermo Fisher Scientific-FEI) measurement tools, and/or via photographs of specimens taken with an optical stereomicroscope (Leica M 205C) connected to a camera (Leica DFC 420C), using tools of the Leica Application Suite v. 4.13.

The peratheriine hemi-mandible from La Borie (UM-BRI-17) was compared in detail with hemi-mandibles of *Peratherium elegans* (Aymard, 1846) (UM-VBO-128, from Valbro) and *Amphiperatherium minutum* (Aymard, 1846) (UM-SNB-508, from Sainte-Néboule), because (i) *Peratherium elegans* is the type species of *Peratherium*, (ii) *A. minutum* was the first species of *Amphiperatherium* with documented intraspecific variation (Crochet 1978), and is the species considered as representing the genus *Amphiperatherium* in the phylogenetic analysis of Ladevèze et al. (2020), and (iii) *Peratherium elegans* and *A. minutum* were the two first valid species included in *Peratherium* by Aymard (1850, p. 83). These two specimens have been illustrated elsewhere (Crochet 1978, 2016). The maximum anteroposterior length

and mediolateral width of each anterior and posterior lower molar alveolus was measured. The anteroposterior alveolus length was taken parallel to the anteroposterior axis of the molar row, and the mediolateral alveolus width was taken perpendicular to the anteroposterior alveolus length.

We accounted for intraspecific variation in the descriptions of dental material based on comparisons with the variation ranges of morphological characters and of size described in the literature for other marsupialiforms, such as *Peradectes* species (Gernelle et al. 2024), *Pucadelphys andinus* Marshall & Muizon, 1988 (Ladevèze et al. 2011), and *Peratherium constans* and *Peratherium elegans* (Ladevèze et al. 2012). Because stylar cusps are often doubled in some peratheriine species, we illustrate the positioning of these additional stylar cusps in Figure 3A-B. Height relationships of stylar cusps were obtained based on upper molars with stylar cusps that were preserved with limited and homogeneous wear.

We employed three measurement methods for the mesiodistal length of upper molars, all taken in occlusal view, parallel to the paracone – metacone axis (Figure 3B): (i) the stylar shelf length (sL), which corresponds to the maximum length of upper molars (sL = L); (ii) the talon length (tL), which was taken at the level of the base of the lingual edge of paracone – metacone, always labial to the conules (the talon is sometimes easily distinguishable from the stylar shelf by a distal emargination; Figure 3B); and (iii) the protocone length (pL), which was taken at the level of the apex of the protocone. We also introduce two measurement methods for the labiolingual width of upper molars, taken perpendicular to the paracone – metacone axis (Figure 3B): (iv) the talon width (tW), which extends from the level of the talon length segment to the lingualmost point of the lingual edge of the protocone; and (v) the protocone width (pW), which is the distance between the labialmost point of the protocone apex and the lingualmost point of the lingual edge of the protocone. We performed these five measurements on upper molars of *Peratherium musivum* sp. nov., and on upper molar samples of the type series of *Peratherium constans* (in addition to the single M3 of *Peratherium constans* reported from Fordones, in Corbières; Marandat 1991: pl. 1, fig. 6; Gernelle et al. 2024) and *Peratherium maximum* comb. nov., including the holotype specimens of these three species. The sL/tL, sL/pL, tL/pL, and tW/pW ratios were further calculated (see Supplemental material 1) and compared via Welch's *t*-test (see below for statistical procedure performed).

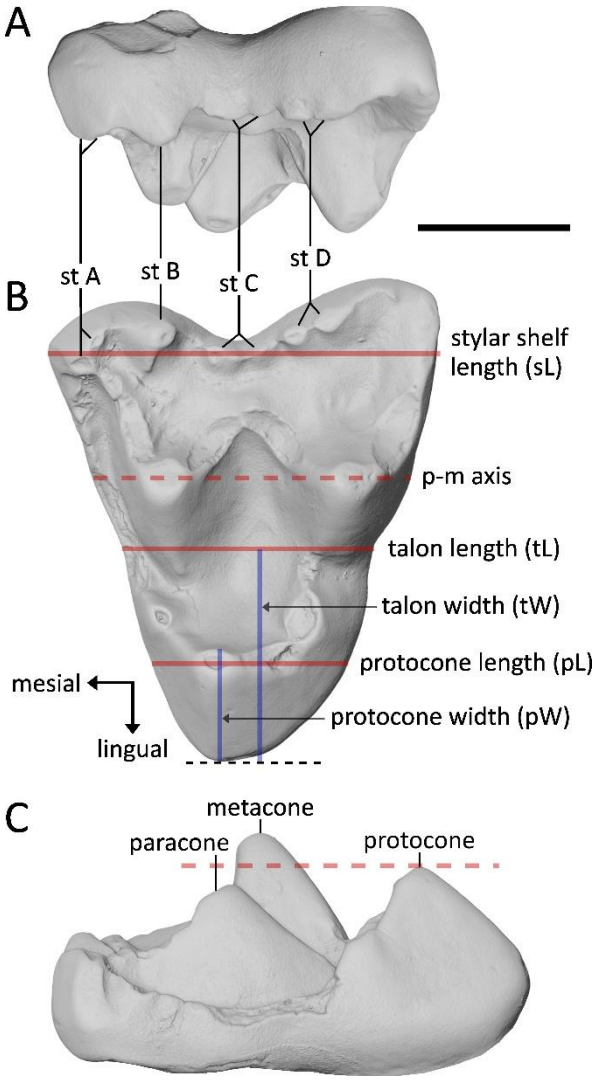


**Figure 3.** Measurement methods of mesiodistal length (sL, tL, pL) and labiolingual width (tW, pW) of peratheriine upper molars introduced in this study, with the positioning of stylar cusps and main cusps, illustrated on the left M3 MNHN.F.CB1252, *Peratherium maximum* comb. nov. from Condé-en-Brie (~MP8+9, Paris Basin), in labial (A), occlusal (B), and mesial (C) views. The arrows indicating the mesial and lingual sides concern the occlusal view (B). The red dashed line in the mesial view (C) is used to compare the heights of the main cusps. Scale bar equals 1 mm. Abbreviations: p-m axis, paracone – metacone axis; st, stylar cusp.

### Quantitative analysis based on isolated lower molars

All isolated lower molars of *Peratherium maximum* comb. nov. from Condé-en-Brie, from the MNHN Palaeontology collection, reviewed by one of us (KG), were attributed to a given locus (m1 to m4) and measured. In addition to the measured length (L), width (W), and width of the talonid (tlW), the approximate surface area of lower molars (S) was calculated with the

formula: S = L/2 * trW + L/2 * tlW, where trW represents the labiolingual width of the trigonid. In fact, (i) the width of the trigonid and of the talonid can differ between molar loci, and (ii) the trigonid and talonid are here assumed to represent approximately half of the total molar length each in early peratheriines. Finally, the relative labiolingual width of the talonid (tlWr) was calculated comparing the talonid width to the approximate surface, as follows: tlWr = tlW/S. Detailed measurements of L, W, trW, and tlW, and calculated values of L/W ratios and tlWr are available in Supplemental material 2. Statistical analysis of the data was done using the R software environment (v.4.3.3; R Core Team 2024). Welch's ANOVA (*W*-test) were performed in order to detect if one or more significant differences occur between means of a given descriptive variable, between lower molar loci (as recommended in Delacre et al. 2019). Multiple comparisons testing was carried out using Games-Howell post-hoc tests, as recommended in Ruxton and Beauchamp (2008), in order to identify which pairs of lower molar loci significantly differ ($P < 0.05$) in length, width and approximate surface area, and additionally in both absolute and relative width of the talonid. Results of the Games-Howell tests are available in Supplemental material 3. The Welch's ANOVA and Games-Howell post-hoc tests were conducted with the function *oneway* of the R package *userfriendlyscience* (Peters 2017). Boxplots were produced using the R package *ggplot2* (Wickham 2016). For each molar locus, all values (including talonid width values) were normally distributed with the exception of the width of m3 (Shapiro-Wilk normality test; $W = 0.84$, $P = 0.018$) and the relative width of the talonid of m3 (Shapiro-Wilk normality test; $W = 0.87$, $P = 0.046$).

## Systematic Palaeontology

Metatheria Huxley, 1880

Marsupialiformes Vullo, Gheerbrant, Muizon & Néraudeau, 2009

Notometatheria Kirsch, Lapointe & Springer, 1997

Herpetotheriidae (Trouessart, 1879)

Peratheriinae Ladevèze, Selva & Muizon, 2020

*Peratherium* Aymard, 1850

### *Remark on generic abbreviation*

We use the abbreviation '*Pt.*' for the genus *Peratherium* in order to avoid confusion with species of the genus *Peradectes*, the latter being mentioned for comparative purposes in this

study. In fact, the type species of these genera have the same species name: *Peratherium elegans* and *Peradectes elegans* Matthew & Granger, 1921.

### ***Peratherium musivum*** sp. nov.

**LSID** urn:lsid:zoobank.org:act:7BC0CE7D-3D4C-46E2-AD86-4E56716F799A

Figures 4A-B, 4E-G, 4I-M, 4P, 5A-M

1980 - *Amphiperatherium* sp. indet. 2 in Crochet p. 137-138 (in part, specimens from Soissons and Rians).

1980 - *Peratherium* sp. indet. 1 in Crochet p. 213-214, fig. 237 (in part, specimen from Soissons).

1981 - *Amphiperatherium* cf. *maximum* Crochet in Godinot p. 54-55, figs. 4c, f.

1981 - *Amphiperatherium goethei* Crochet in Godinot p. 54, fig. 4d.

1991 - *Amphiperatherium* sp. indet. cf. *A.* cf. *maximum* in Godinot, 1981, in Marandat p. 72-73, pl. 1, fig. 15.

1996 - *Amphiperatherium* cf. *maximum* Crochet in Louis p. 94, pl. 2, fig. 6.

#### *Nomenclatural remark*

This new species must be referred to as *Peratherium musivum* Gernelle, 2024, following the article 50.1 and the recommendation 50A concerning multiple authors of the International Code of Zoological Nomenclature (ICZN 1999: 52).

#### *Remark on generic attribution*

The rationale for the attribution of this new species to the genus *Peratherium* is detailed in discussion.

#### *Etymology*

From the latin word '*musivum*' meaning 'mosaic'. Refers to: (i) the size of the species, larger than the earliest peratheriine species *Peratherium constans* and smaller than the younger '*Amphiperatherium*' *maximum*, purported earliest *Amphiperatherium* species; and (ii) the morphological characters partly shared with *Pt. constans* and/or '*A.*' *maximum*.

#### *Holotype*

MNHN.F.SN122, right M3 (Figures 4I-K, P; Crochet 1980: fig. 237). A 3D surface model of this specimen is available on the online platform MorphoMuseuM (Lebrun and Orliac 2016).

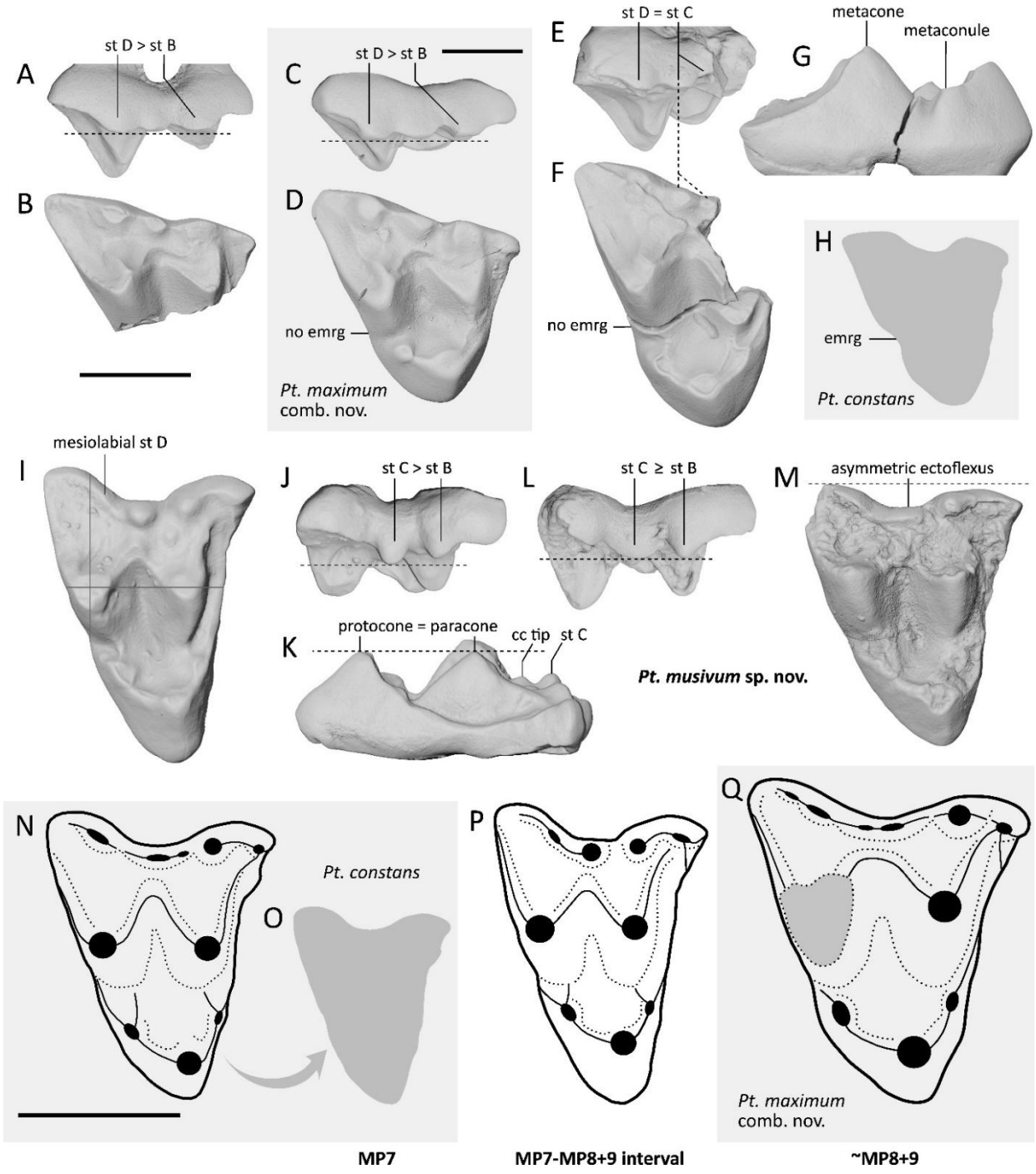


**Figure 4.** Upper molars of *Peratherium musivum* sp. nov. from MP7-MP8+9 interval localities of Rians (Provence) and Soissons (type locality; Paris Basin, Aisne), compared with upper molars of *Pt. constans* Teilhard de Chardin, 1927, from Dormaal (MP7; Belgium) and of *Pt. maximum* comb. nov., from Pourcy (MP7-MP8+9 interval; Paris Basin) and Condé-en-Brie (~MP8+9; Paris Basin). A-B. MNHN.F.RI296, labial half of right M1 of *Pt. musivum* sp. nov. in labial (A) and occlusal (B) views. C-D. MNHN.F.PY18001, left M1 of *Pt. maximum* comb. nov. in labial (C) and occlusal (D) reversed views. E-G. MNHN.F.RI220, fragment of left M2 of *Pt. musivum* sp. nov., which lacks the paracone and parastylar wing, in labial (E), occlusal (F) and distal (G) reversed views. H. Outline of IRSNB-M-1, right M2 holotype of *Pt. constans*, in occlusal view. Adapted from Ladevèze et al. (2012: fig. 1a). I-K. Holotype of

*Pt. musivum* sp. nov., MNHN.F.SN122, right M3 in occlusal (I), labial (J) and mesial (K) views. L-M. MNHN.F.SN14, left M3 of *Pt. musivum* sp. nov. in labial (L) and occlusal (M) reversed views. N-O. Interpretative drawing (N) and outline (O) (differing in scale) of reversed occlusal view of IRSNB-M-2030, left M3 of *Pt. constans*, adapted from Ladevèze et al. (2012: fig. 4Cb). P. Interpretative drawing of occlusal view of MNHN.F.SN122, right M3 holotype of *Pt. musivum* sp. nov. Q. Interpretative drawing of occlusal view of MNHN.F.CB198, right M3 holotype of *Pt. maximum* comb. nov., based on a cast. Light grey boxes concern *Pt. constans* and *Pt. maximum* comb. nov. specimens. Scale bars equal 1 mm. The scale bar below B. applies to all except C.-D. and N. Abbreviations: cc tip, centrocrista tip; emrg, distal emargination; st, stylar cusp.

***Type locality***

Soissons (Aisne, Paris Basin, northern France).

***Other localities***

Le Clot (Corbières), Fournes (Minervois), Rians (Provence), all in southern France; Pourcy (Paris Basin) in northern France.

***Age***

MP7-MP8+9 interval; from between the PETM and ETM2 (~55 Ma), based on the age of Le Clot (Yans et al. 2014), to at least consecutively to the ETM2 (~54 Ma), based on the age of Fournes (Noiret et al. 2016). Biozones PE II to PE III (Hooker 1996a; Marandat et al. 2012).

***Material***

Additional material from Soissons: left M3 (MNHN.F.SN14), right m1 (MNHN.F.SN2507; Louis 1996: pl. 2, fig. 6).

Material from Le Clot: trigonid of right m2 or m3 (UM-CLO-50), fragmentary talonid of right m2 or m3 (UM-CLO-51).

Material from Fournes: right m3 (UM-FNR-23; Marandat 1991: pl. 1, fig. 15).

Material from Rians: stylar shelf of right M1 (MNHN.F.RI296; Godinot 1981: fig. 4c), distal fragment of left M2 (MNHN.F.RI220), left m1 (MNHN.F.RI385; Godinot 1981: fig. 4d), right m2 (MNHN.F.RI368; Godinot 1981: fig. 4f). 3D surface models of the four specimens from Rians are available on MorphoMuseuM.

Material from Pourcy: right m2 or m3 with fragmentary talonid (MNHN.F.PY18003).

***Differential diagnosis***

Peratheriine markedly larger than *Pt. constans* (~ twice the surface area of molars) and *Pt. matronense* Crochet, 1979, and markedly smaller than *Pt. maximum* comb. nov. Differs from

*Pt. constans*, *Pt. matronense*, and *Pt. maximum* comb. nov. in having stylar cusp C apex more ventral than stylar cusp B and D apices on M3 (or as ventral for stylar cusp B). Further differs from *Pt. constans* and *Pt. matronense* in having (i) stylar cusp D apex more ventral than stylar cusp B and C apices on M1; and (ii) lingual edge of the hypoconulid much longer than its labial edge on m1. Further differs from *Pt. constans* in (i) lacking the deep distal emargination of M2 crown in occlusal view; and probably (ii) in having a relatively slightly larger protocone – talonid functional complex. Further differs from most *Pt. maximum* comb. nov. specimens in lacking the frequent duplication of stylar cusp D.

**Comparative description**

***Upper molars***

Only four upper molars are reported so far. M1 is only documented by the right labial fragment MNHN.F.RI296, which preserves a worn paracone, metacone and centrocrista (Figure 4A-B). As on all peratheriine upper molars, including the other upper molar loci of *Pt. musivum* sp. nov., the centrocrista is strongly V-shaped, and its most labial point, lingual to stylar cusp C, does not reach the stylar line. Along the stylar line, only stylar cusps C and D, and the labial edge of stylar cusp B are well preserved, the rest of stylar cusp B being worn (Figure 4B). The labiolingually shallow metastylar area, in addition to the short preparacrista connected to stylar cusp B, are characteristic of M1 (Figure 4A). The M1 is similar in length to the two M3s (Table 1). Such similar length values between molar loci also occur in other early Eocene peratheriine species (e.g., *Pt. monspeliense* Crochet, 1979; Crochet 1980: table 37). Similar to M1 of the larger *Pt. maximum* comb. nov. (e.g., MNHN.F.PY18001 from Pourcy, here reported; Figure 4C-D), the ectoflexus is mesiodistally short, and its most lingual point is slightly mesiolabial to stylar cusp C, the latter being intermediate in position between stylar cusps B and D on the stylar line. Moreover, the height relationships of stylar cusps of the M1 of the two species are the same, as follows: D > C > B >> A (see also Crochet 1980: fig. 106a, when correctly oriented). Stylar cusp B is thus not dominant in height on M1 in *Pt. musivum* sp. nov. and *Pt. maximum* comb. nov. (see also Crochet 1980, p. 101, bottom). The same height relationships of stylar cusps B and D are recovered on M1s of *A. bastbergense* and *A. fontense* (pers. obs. KG; Crochet 1979, p. 372). Stylar cusps B and D are subequal in length, and stylar cusp C is shorter on MNHN.F.RI296. The distal crest of stylar cusp D is long. From the distolabial corner of the crown to the base of the metacone, the distal edge of the stylar shelf is straight, as in *Pt. maximum* comb. nov., and unlike most *Pt. constans*

(Ladevèze et al. 2012: fig. 5A-C) and *Pt. matronense* (Crochet 1980: fig. 157b) M1s, in which it is curved.

**Table 1**.

| Specimen | Locus | L (mm) | W (mm) | L/W |
|---|---|---|---|---|
| MNHN.F.RI296 | M1 | 1.91 | - | - |
| MNHN.F.RI220 | M2 | - | 2.40 | - |
| MNHN.F.SN122 | M3 | 1.91 | 2.67 | 0.72 |
| MNHN.F.SN14 | M3 | 1.97 | 2.37 | 0.83 |

Measurements of upper molars of *Peratherium musivum* sp. nov. from the MP7-MP8+9 interval localities of Rians (southern France) and Soissons (northern France). Abbreviations: L, length; W, width.

The unique M2 of *Pt. musivum* sp. nov. is a relatively large distal fragment of upper molar, which lacks the mesial part of the stylar shelf; i.e., the paracone, parastylar wing, and stylar cusps A and B (MNHN.F.RI220; Figure 4E-G). Because the paracone is not preserved in MNHN.F.RI220, the most accurate orientation of this specimen (depending on the paracone – metacone axis) is unclear. It is here figured in the position in which the paraconule is slightly more labial than the metaconule (Figure 4F), as on most early Eocene peratheriine upper molars when the paracone and metacone are aligned (pers. obs. KG). MNHN.F.RI220 is also damaged between the stylar shelf and the talon; it was thus probably slightly narrower than measured here (Table 1). This specimen is similar in width to the narrowest of the two M3s (MNHN.F.SN14; Table 1). MNHN.F.RI220 most likely represents an M2 rather than an M1 or an M3, because the distance between the metacone apex and stylar cusp D (i.e., the labiolingual width of the metastylar wing) is greater than in M1; thus the postmetacrista is longer (Figure 4F vs Figure 4B), and the talon is relatively mesiodistally longer and more rounded than on M3 (Figure 4F vs Figure 4I, M). Furthermore, the ectoflexus is deep labial to stylar cusp C, as on M2 of *Pt. constans* (Figure 4H), and unlike on peratheriine M1s (see above). The protocone is lower than the metacone (Figure 4G). A preparaconular crista and a short postparaconular crista reaching the lingual part of the base of the paracone are present. The metaconule has a premetaconular crista and a faint postmetaconular crista distinguishable in distal view, in which the fossa between the metaconule and the metacone base appears deep

(Figure 4G). In occlusal view, the distal emargination of the crown is lacking on MNHN.F.RI220, as on M2 of *Pt. maximum* comb. nov. (pers. obs. [KG] of the specimen figured in Crochet 1980: fig. 107) and of *Pt. matronense* (Crochet 1980: fig. 158b), and unlike on M2 of *Pt. constans* (Figure 4F vs Figure 4H). Although this trait is subject to intraspecific variation in peradectid species (Gernelle et al. 2024), the presence of a distal emargination on unworn upper molars is diagnostic of several peratheriine species such as *Pt. constans* (on M1 and M2) and *Pt. bretouense* Crochet, 1979 (pers. obs. [KG] of their type series, from Dormaal and Le Bretou, respectively). Labial to the centrocrista, stylar cusp C is doubled. Of the two small cusps in the C position (i.e., slightly mesiolabial to slightly distolabial to the most labial point of the centrocrista; Clemens 1966, p. 3), the distal one is larger (i.e., longer, wider and higher) (Figure 4E-F). This distal cusp is as high as stylar cusp D (Figure 4E), but, as on M1, the latter is mesiodistally longer. Stylar cusp D is directly labial to the metacone apex, also as on M1.

Two M3s are documented; both are from Soissons. They are larger than the M3s of *Pt. constans* and smaller than the M3s of *Pt. maximum* comb. nov. (Figure 4O vs Figure 4P vs Figure 4Q). MNHN.F.SN14 is slightly mesiodistally longer and labiolingually narrower than the holotype MNHN.F.SN122 (Table 1). The procumbent protocone of MNHN.F.SN122 is as high as the paracone in distal view (Figure 4K) (the protocone of MNHN.F.SN14 is worn). The protocone of MNHN.F.SN122 is labiolingually wider than that of MNHN.F.SN14 (Figure 4I vs Figure 4M). The metacone is the highest of the three principal cusps. It is mesiodistally longer than the paracone. Note that the principal cusps and conules are worn on the holotype, so that only the outlines of the conules are preserved. The conules have the same relative sizes as on upper molars of *Pt. constans* (Figure 4N vs Figure 4P) (this is also true for the conules of the M2). The most labial point of the centrocrista forms an accessory cusp, which is lower than the almost adjacent stylar cusp C (Figure 4K). Such an accessory cusp is also observed on M3 of *Pt. constans* (Ladevèze et al. 2012: fig. 5H). A faint distal emargination is present on the crown of the holotype, in occlusal view. The labial end of the long preparacrista is directed towards stylar cusp A, as on M3 of other peratheriine species (e.g., Figure 4N, P-Q; Ladevèze et al. 2012: fig. 7a-b). The postmetacrista is transversely oriented on M3. Stylar cusp A is strictly mesial to stylar cusp B on MNHN.F.SN14 (Figure 4M), whereas it is mesiolabial to stylar cusp B on the holotype (Figure 4I, P). Stylar cusps A and B are connected by a crest. The distance between stylar cusps A and B does not differ from that of other peratheriine species (Figure 4P vs Figure 4N, Q; *contra* Crochet 1980, p.

214). Stylar cusp B is positioned directly labially to the paracone apex, as in all known early Eocene herpetotheriids. On both M3s of *Pt. musivum* sp. nov., stylar cusps B and C are not connected, while stylar cusps C and D are connected by a crest (Figure 4M, P), similar to, for example, *A. bastbergense* M3s (Crochet 1979: fig. 8). Stylar cusps B and C are much smaller than the paracone. Stylar cusp C is conical on MNHN.F.SN122 (Figure 4J), and crescentiform on MNHN.F.SN14 (Figure 4L). Both M3s have a high stylar cusp C, of which the apex is more ventral than the apex of stylar cusp B on MNHN.F.SN122 (Figure 4J), and as ventral as the apex of stylar cusp B on MNHN.F.SN14 (Figure 4L). The height relationships of stylar cusps of *Pt. musivum* sp. nov. M3, which differs from the ones of the M1, are as follows: C ≥ B >> D ≥ A. In the same way, the stylar height relationships differ between successive upper molar loci in other peratheriine species, such as the similarly-sized *A. bastbergense* Crochet, 1979, and *A. fontense* Crochet, 1979 (Crochet 1979, p. 372). By contrast, stylar cusp B is dominant in height on the M3 of *Pt. constans* and of *Pt. maximum* comb. nov. (e.g., Figure 3A; Crochet 1980: fig. 108a). Although stylar cusp D is long in *Pt. musivum* sp. nov., it is not doubled, unlike stylar cusp D of various upper molars of *Pt. maximum* comb. nov. (Figure 4P vs Figures 3B, 4Q), and rare upper molars of *Pt. constans* (pers. obs. [KG] of a cast of the M3 IRSNB-M-1331). Stylar cusp D is positioned mesiolabially to the metacone apex on MNHN.F.SN122, and is directly labial to the metacone apex on MNHN.F.SN14 (Figure 4P vs Figure 4M). A similar variation in the relative positioning of stylar cusp D exists also on M3 of *Pt. maximum* comb. nov. (pers. obs. KG). The ectoflexus of M3 is deep, long and asymmetric. Because the metastylar wing is much more labially projected than the parastylar wing on MNHN.F.SN122 (Figure 4I), the asymmetry of its ectoflexus is more pronounced than that of MNHN.F.SN14 (Figure 4M). M4 is not yet known.

***Lower molars***

As for lower molars, the low number of available measurements shows a relative mesiodistal elongation from m1 to m3 (Table 2), whereas there is no apparent elongation of upper molars from M1 to M3 (Table 1). The talonid is similarly sized from m1 to m3, but the trigonid labiolingually widens (Table 2), and the trigonid cuspids enlarge (e.g., Figure 5A, D, F). The protoconid is the largest cuspid. The paraconid of the m1 MNHN.F.SN2507 is broken (Figure 5A-B), and the paraconid of the m1 MNHN.F.RI385 is worn (Figure 5H). The precingulid is weakly developed on m1; it is only mesial to the lingual segment of the paracristid on MNHN.F.SN2507, and it is absent on MNHN.F.RI385 (Figure 5H). A reduced precingulid also occurs at least on one m1 of *Pt. constans* (Ladevèze et al. 2012: fig. 6Ca), and on other

lower molar loci of this species (Ladevèze et al. 2012: fig. 6Ga). Although the morphology of the precingulid varies between m2 and m3 specimens, this structure is limited to the mesial edge of the trigonid; its labial extremity terminates mesiolabial to the protoconid apex (i.e., the protoconid is not surrounded by a cingulid). The paracristid is longer than the protocristid. In labial view, the preprotocristid is not as curved as in peradectids (Figure 5B). The distal flank of the paraconid is developed, so that the surface area occupied by the paraconid in occlusal view is greater than the surface area occupied by the metaconid. The metaconid is longer than the paraconid on m1 and m2 (e.g., Figure 5E), and is as long as the paraconid on m3 (Figure 5G). The metaconid is positioned almost strictly lingually to the protoconid on all lower molars,

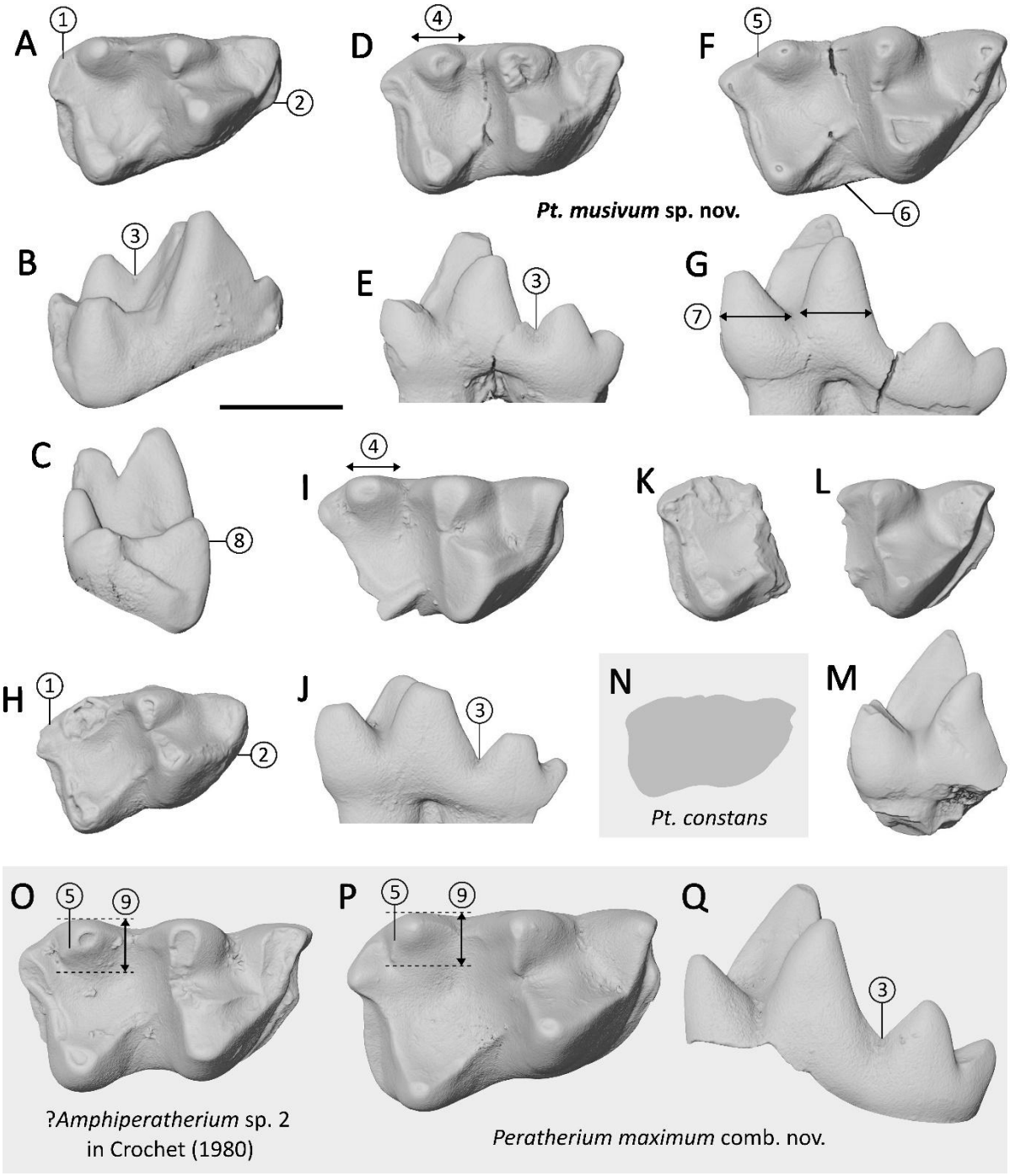


**Figure 5.** Lower molars of *Peratherium musivum* sp. nov. from MP7-MP8+9 interval localities of Soissons and Pourcy, in the Paris Basin, and Rians, Fournes and Le Clot in southern France (A-M), compared with lower molars of selected peratheriines (N-Q). A-C. MNHN.F.SN2507, right m1 in occlusal (A), labial (B) and distal (C) views. D-E. MNHN.F.RI368, right m2 in occlusal (D) and lingual (E) views. F-G. UM-FNR-23, right m3 in occlusal (F) and lingual (G) views. H. MNHN.F.RI385, left m1 in reversed occlusal view. I-J. MNHN.F.PY18003, partial right m2 or m3 in occlusal (I) and lingual (J) views. K. UM-CLO-51, talonid of right m2 or m3 in occlusal view. L-M. UM-CLO-50, trigonid of right m2 or m3 in occlusal (L) and lingual (M) views. N. Outline of a complete left m2 of *Pt. constans* Teilhard de Chardin, 1927, from Le Clot, in reversed occlusal view. O. MNHN.F.AV6789,

left m3 of ?*Amphiperatherium* sp. indet. 2 in Crochet (1980), in reversed occlusal view. P-Q. MNHN.F.PY18002, left m2 of *Pt. maximum* comb. nov., in occlusal (P) and lingual (Q) reversed views. Light grey boxes concern *Pt. constans*, ?*Amphiperatherium* sp. indet. 2 and *Pt. maximum* comb. nov. specimens. Scale bar equals 1 mm. Significance of labelled characters studied in the main text: 1. Long lingual edge of the hypoconulid (asymmetric hypoconulid). 2. Weak to absent precingulid. 3. Short and/or shallow metaconid – entoconid notch. 4. Long entoconid. 5. Postentocristid. 6. Wide hypoflexid. 7. Paraconid as long as metaconid. 8. Hypoconid lower than entoconid. 9. Large (wide and long) and lingually convex entoconid.

as in most herpetotheriid metatherians (e.g., Gernelle et al. 2024: table 6). The lingual opening of the trigonid is as high as the lingual opening of the talonid on m1 and m2 (Figure 5E). This character is indicative of herpetotheriids among Laurasian marsupialiforms (e.g., Gernelle et al. 2024: table 6; pers. obs. KG). The lingual opening of the trigonid is higher than the one of the talonid on m3 (Figure 5G), as in *Pt. maximum* comb. nov. (*contra* Marandat 1991, p. 72). A labial emargination of the crown is present on the m1 MNHN.F.RI385 (Figure 5H), and is absent on MNHN.F.SN2507 (Figure 5A). The hypoflexid widens from m1 to m3, so that the labial emargination is also absent on m3 (Figure 5F).

The cristid obliqua is straight and mesially ends labially to the protocristid notch. On the m3 UM-FNR-23, the mesial end of the cristid obliqua is more lingual, closer to the protocristid notch, than on m1, m2, and MNHN.F.PY18003. The hypoconid is not mesiodistally pinched, similar to *Pt. constans* and *Pt. maximum* comb. nov., and unlike, for example, *Pt. elegans* or *A. minutum* (e.g., this study; Ladevèze et al. 2012: fig. 7c-e). The hypoconid apex is positioned labially (Figure 5A) or distolabially (Figure 5D) to the entoconid apex. The entoconid is much higher than the hypoconid on m1 (Figure 5C) and m2, and is only slightly higher than the hypoconid on m3. The entoconid is much mesiodistally longer than the hypoconulid on all specimens (e.g., Figure 5D, I). In labial and lingual views, the entoconid – hypoconulid notch is lower than the metaconid – entoconid notch on m1 and m2 (e.g., Figure 5B, E), and the two notchs are almost as high on m3 (Figure 5G). As a consequence, the m3 UM-FNR-23 is the only lower molar displaying an entoconid with a symmetrical shape in lingual view. It is also the single lower molar of *Pt. musivum* sp. nov. with a labiolingually pinched entoconid, with a sharp postentocristid. The latter cristid has not been described in *Pt. constans* (Ladevèze et al. 2012), but is present in *Pt. maximum* comb. nov. and in ?*Amphiperatherium* sp. 2 in Crochet (1980) from Avenay (Figure 5O-P). On m1, the hypoconulid is relatively labiolingually wider, and with its apex positioned less lingually than

on other molar loci. In particular, the lingual edge of the hypoconulid, adorned by a sharp cristid on MNHN.F.SN2507, is labiolingually longer than its labial edge on m1 (Figure 5A, H), whereas the lingual and labial edges are subequal in length on m2 and on m3 (Figure 5D, F, I, K). This asymmetric morphology of the hypoconulid occurs also on m1 and even m2 (e.g., Figure 5P) of *Pt. maximum* comb. nov. (pers. obs. [KG] of the type series from Condé-en-Brie) but not in *Pt. constans* (e.g., Ladevèze et al. 2012: fig. 4Ea). The distolingual edge of the talonid is less and less curved from m1 to m3 (Figure 5A, D, F).

**Table 2**. Measurements of lower molars of *Peratherium musivum* sp. nov. from the MP7-MP8+9 interval localities of Soissons and Pourcy (northern France), and Rians, Fournes and Le Clot (southern France). *, fragmentary specimen, probably slightly longer than measured. Abbreviations: L, length; tlW, talonid width; trW, trigonid width; W, width.

| Specimen | Locus | L (mm) | W (mm) | L/W | trW (mm) | tlW (mm) |
|---|---|---|---|---|---|---|
| MNHN.F.SN2507 | m1 | 1.90 | 1.24 | 1.53 | 1.03 | 1.22 |
| MNHN.F.RI385 | m1 | 1.73 | 1.19 | 1.45 | 0.99 | 1.15 |
| MNHN.F.RI368 | m2 | 1.98 | 1.24 | 1.60 | 1.09 | 1.23 |
| UM-FNR-23 | m3 | 2.35 | 1.37 | 1.72 | 1.29 | 1.27 |
| MNHN.F.PY18003 | m2 or 3 | 2.04* | - | - | 1.21 | - |
| UM-CLO-50 | m2 or 3 | - | - | - | 1.14 | - |
| UM-CLO-51 | m2 or 3 | - | - | - | - | 1.19 |

The lower molar from Pourcy (MNHN.F.PY18003, Figure 5I-J) is either an m2 or an m3, which are molar loci of *Pt. musivum* sp. nov. with undocumented morphological and size variation. The distolabial part of the talonid (including the hypoconid, postcingulid, and part of the hypoconulid) is lacking on MNHN.F.PY18003. This specimen is much smaller than lower molars of *Pt. maximum* comb. nov., also present in Pourcy (e.g., MNHN.F.PY18002; Figure 5I-J vs Figure 5P-Q). The entoconid is not lingually convex, similarly to other *Pt. musivum* sp. nov. lower molars, which allows us to allocate MNHN.F.PY18003 to this species with more confidence, instead of to *Pt. maximum* comb. nov. It is worth noting that the entoconid is sometimes weakly lingually convex in *Pt. maximum* comb. nov., and occasionally lingually convex in *Pt. constans* (Ladevèze et al. 2012: fig. 4Fa). MNHN.F.PY18003 is closer in mesiodistal length to the single known m2 of *Pt. musivum* sp. nov. (although the length of the latter could be slightly underestimated, due to fragmentation), and is slightly closer to the m3 from Fournes in its absolute trigonid width value (Table 2). The lingual opening of the trigonid much higher than the lingual opening of the talonid

resembles an m3, while the entoconid – hypoconulid notch lower than the metaconid – entoconid notch in lingual view better resembles an m2 (Figure 5J).

The right trigonid and talonid fragments from Le Clot represent two distinct specimens morphologically similar to other lower molars of *Pt. musivum* sp. nov. The labiolingual width of the right trigonid (UM-CLO-50, Figure 5L-M) is closer to the width value of the trigonid of the ascertained m2 (Table 2). The metaconid is intermediate in height between the paraconid and the protoconid, and is slightly longer than the paraconid (Figure 5M); the latter character also resembles the condition seen in the m2. The postmetacristid is long. The precingulid is relatively longer and wider than on other lower molars of *Pt. musivum* sp. nov.; the relative size of this structure is known to vary in other marsupialiform species (e.g., Ladevèze et al. 2012: figs. 6-8). The right isolated talonid (UM-CLO-51, Figure 5K) is fragmented at the level of the entoconid. The hypoconulid projects as distally to the postcristid as in other lower molars of *Pt. musivum* sp. nov. and *Pt. constans*, and the postcingulid is labiolingually long. The hypoconulid is more lingually positioned, and its lingual edge is relatively shorter than on m1. UM-CLO-51 represents either an m2 or an m3. The m4 is not yet known, but its talonid is expected to be less labiolingually wide based on the proportions of m4 in other herpetotheriid species.

**Additional detailed comparisons**

The specimens discussed below which have been attributed to or compared with *Peratherium* sp. indet. 1 in Crochet (1980) are (except MNHN.F.SN122) provisional undetermined peratheriines. The M3 MNHN.F.SN122, holotype of *Peratherium musivum* sp. nov., was attributed to *Peratherium* sp. indet. 1 by Crochet (1980, pp. 213-214), and compared to the M2 or M3 UM-BOUX-28-L (Bouxwiller, ~MP13), which was placed under the same denomination. The paracone is relatively higher on MNHN.F.SN122, subequal to the protocone instead of lower, and not as low compared to the metacone. Furthermore, stylar cusp C is much higher than stylar cusp D on M3s of *Pt. musivum* sp. nov., whereas stylar cusp C is close in height to stylar cusp D on the specimen from Bouxwiller (pers. obs. [KG] of a cast of UM-BOUX-28-L).

A mesially worn M3 from Azillanet (Minervois, MP10), comparable to MNHN.F.SN122 in size and occlusal outline, was attributed to *Peratherium* cf. *Peratherium* sp. indet. 1 in Crochet (1980) (UM-AZI-1-6; Marandat 1986: pl. 1, fig. 3). *Peratherium musivum* sp. nov.

differs notably in having stylar cusp C dominant in size over stylar cusp B, instead of the opposite.

An M3 from Vielase (UM-VIE-104; Quercy, ?MP10-11 interval) was listed as *Peratherium* indet. aff. *Peratherium* sp. indet. 1 in Crochet (1980) (Legendre et al. 1992), possibly because it is similar in size to MNHN.F.SN122, and because stylar cusp C is higher than stylar cusp B. The M3s of *Pt. musivum* sp. nov. differ in the relatively labiolingually narrower stylar shelf, compared to the talon; in having stylar cusp C connected by a crest to stylar cusp D, instead of connected to stylar cusp B on UM-VIE-104; and because stylar cusp D is the lowest stylar cusp, instead of being clearly dominant over the other stylar cusps on UM-VIE-104.

An M2 of *Peratherium* sp. 1 from the Bracklesham Group (Southern England), Dummer's Copse locality DC5iii (MP10) (specimen NHMUK.PV.M50180), was also compared to *Peratherium* sp. indet. 1 in Crochet (1980) from Soissons (i.e., MNHN.F.SN122) (Hooker 1996b, pp. 142-143, pl. 1, fig. 4). The two specimens share a 'larger protocone lobe' according to Hooker (1996b), although they do not represent the same molar locus. The proportions of the talon of the two specimens actually differ greatly, the talon of MNHN.F.SN122 being relatively labiolingually wider than the talon of the English specimen. The protocone of both specimens is not particularly relatively larger than the protocone of M2 or M3 belonging to other early Eocene peratheriines (*contra* Hooker 1996b). This is also true when considering the protocone of the *Pt. musivum* sp. nov. M2 MNHN.F.RI220, which is relatively larger than the one of the M3 MNHN.F.SN122.

An M3 from Avenay of *Amphiperatherium* sp. indet. 1 in Crochet (1980) (MNHN.F.AV18005, Crochet 1980: fig. 41) displays a stylar cusp C that is higher than stylar cusps B and D (pers. obs. KG), as in *Pt. musivum* sp. nov. Such a low stylar cusp B would be indicative of the genus *Amphiperatherium* according to Hooker et al. (2008). Molars of *Pt. musivum* sp. nov. are much larger than those of *Amphiperatherium* sp. indet. 1, MNHN.F.AV18005 being approximately as small as M3s of *Pt. constans* (Crochet 1980: table 6).

The m1 MNHN.F.SN2507 from Soissons was initially attributed to *Amphiperatherium* sp. indet. 2 by Crochet (1980, pp. 137-138), and specimens from Rians here reallocated to *Pt. musivum* sp. nov. were suggested as being possibly related to *Amphiperatherium* sp. indet. 2 (*sensu* Crochet 1980) by Godinot (1981, p. 55). *Amphiperatherium* sp. indet. 2 includes specimens smaller than '*A.*' *maximum* according to Crochet (1980). The only specimen found

in the MNHN collections which was still referred to this taxon is the m3 MNHN.F.AV6789 (Figure 5O; L = 2.38 mm; W = 1.44 mm; trW = 1.33 mm in occlusal view). Interestingly, the widest lower molar of *Pt. musivum* sp. nov. (UM-FNR-23) is slightly smaller than the specimen from Avenay, while one relatively small m2 of *Pt. maximum* comb. nov. from Pourcy (MNHN.F.PY18000, see below) is slightly larger. It should be mentioned that MNHN.F.AV6789 is distolabially damaged; it was thus probably slightly larger. The entoconid of lower molars of *Pt. musivum* sp. nov. has a straight lingual edge, whereas the lingual edge of the entoconid is convex on MNHN.F.AV6789 (Figure 5O), similar to most m2s and m3s of *Pt. maximum* comb. nov. (e.g., Figure 5P).

Molars of *Pt. musivum* sp. nov. differ from those of *Peratherium* cf. *monspeliense* from Fournes and La Gasque (Minervois; Marandat 1991, pp. 70-71), notably in being markedly larger and in having a stylar cusp B that is non-dominant in height.

*Peratherium musivum* sp. nov. is closer in size to the large peratheriine *A. bastbergense*, but is still markedly smaller (Tables 1-2 vs Crochet 1980: table 15) (in turn, most molar loci are smaller in *A. bastbergense* than in '*A.*' *maximum*, based on available mean values). M3s of *Pt. musivum* sp. nov. have stylar cusp C as high as or higher than stylar cusp B instead of a dominant stylar cusp B (e.g., Figure 4J, L vs Crochet 1980: fig. 114a), and all lower molars, including the talonid fragment from Le Clot (UM-CLO-51; Figure 5K) have a relatively mesiodistally shorter hypoconulid (e.g., Figure 5A, D vs Crochet 1980: figs. 116-117).

*Peratherium musivum* sp. nov. differs from the early Eocene herpetotheriines such as the *Herpetotherium* species (*sensu* Korth 2008; Williamson et al. 2012) *H. knighti* (McGrew, 1959) and *H. edwardi* (Gazin, 1952), notably in having: (i) M3 with a deeper ectoflexus; (ii) M1 to M3 with a stylar cusp D most often directly labial instead of always mesiolabial to the metacone apex; (iii) stylar cusp C dominant in height on M3; and (iv) lower molars with an entoconid not convex lingually (e.g., Gazin 1952: pl. 1, figs. 3-4; McGrew et al. 1959: fig. 3; Krishtalka and Stucky 1983b: figs. 1-2; Murphey et al. 2018: figs. 11-12; pers. obs. [KG] of casts of the *H. knighti* holotype AMNH 55684, and of the *H. edwardi* holotype USNM 19206 and specimen USNM 19200).

### ***Peratherium* cf. *musivum*** sp. nov.

1998 - *Amphiperatherium maximum* Crochet? in Hooker p. 449.

2005 - *Amphiperatherium maximum* Crochet? in Hooker et al. p. 84.

2010 - *Amphiperatherium* sp. 2 in Hooker p. 17, fig. 8q.

***Locality and age***

Abbey Wood (England, London); MP7-MP8+9 interval, PE III biozone, 55.12 Ma according to Hooker (2010).

***Material***

right p2 (NHMUK.PV.M60002; Hooker 2010: fig. 8q).

***Remarks***

Lower premolars of peratheriine species differ mostly in size. Hooker (2010, p. 17) stated that the large procumbent peratheriine p2 from Abbey Wood (NHMUK.PV.M60002) is possibly about the right size (L = 1.90 mm, W = 0.66 mm; data from Hooker [2010]) to belong to *Pt. maximum* comb. nov., then documented solely by isolated molars. The p2 of *Pt. maximum* comb. nov. from La Borie (see below; Figure 6A) is much wider and slightly longer, and its p3 is even larger (Table 3). In particular, the width value of NHMUK.PV.M60002 is closer to the one of the p2 of the small *Amphiperatherium* sp. 1 from Abbey Wood (Hooker 2010: fig. 8n-p; L = 1.30 mm, W = 0.52 mm), of which the molars are somewhat close in size to those of *Pt. constans* (= *A.* '*brabantense*') and *Pt. matronense* (Hooker 2010, p. 16), than to the one of *Pt. maximum* comb. nov. (W = 0.91 mm; Table 3). Furthermore, the observed range of the width of the three lower premolars of *Amphiperatherium* sp. 1 from Abbey Wood is low (Hooker 2010, p. 16). However, NHMUK.PV.60002 is closer in length to the *Pt. maximum* comb. nov. p2 than to the *Amphiperatherium* sp. 1 p2. The lower premolar from Abbey Wood could thus represent *Pt. musivum* sp. nov., which is smaller than *Pt. maximum* comb. nov., and of which the description is solely based on isolated molars. For this last reason, the specimen from Abbey Wood is left in open nomenclature.

## ***Peratherium maximum*** (Crochet, 1979) comb. nov.

Figures 4C-D, 4Q, 5P-Q, 6A, 7D-K

***Remark on specimens studied***

Only the new hemi-mandible from La Borie is described and compared below. The allocated material from Pourcy is compared with *Pt. musivum* sp. nov. above. All lower molars and 18 upper molars of *Pt. maximum* comb. nov. from the type locality (Condé-en-Brie) are studied

in the Results section. The redefinition and thorough revision of *Pt. maximum* comb. nov., also abundant in various ~MP8+9 Paris Basin localities, and present in slightly younger localities (Crochet 1980; Louis and Laurain 1983; Hooker 1996b), is beyond the scope of this study.

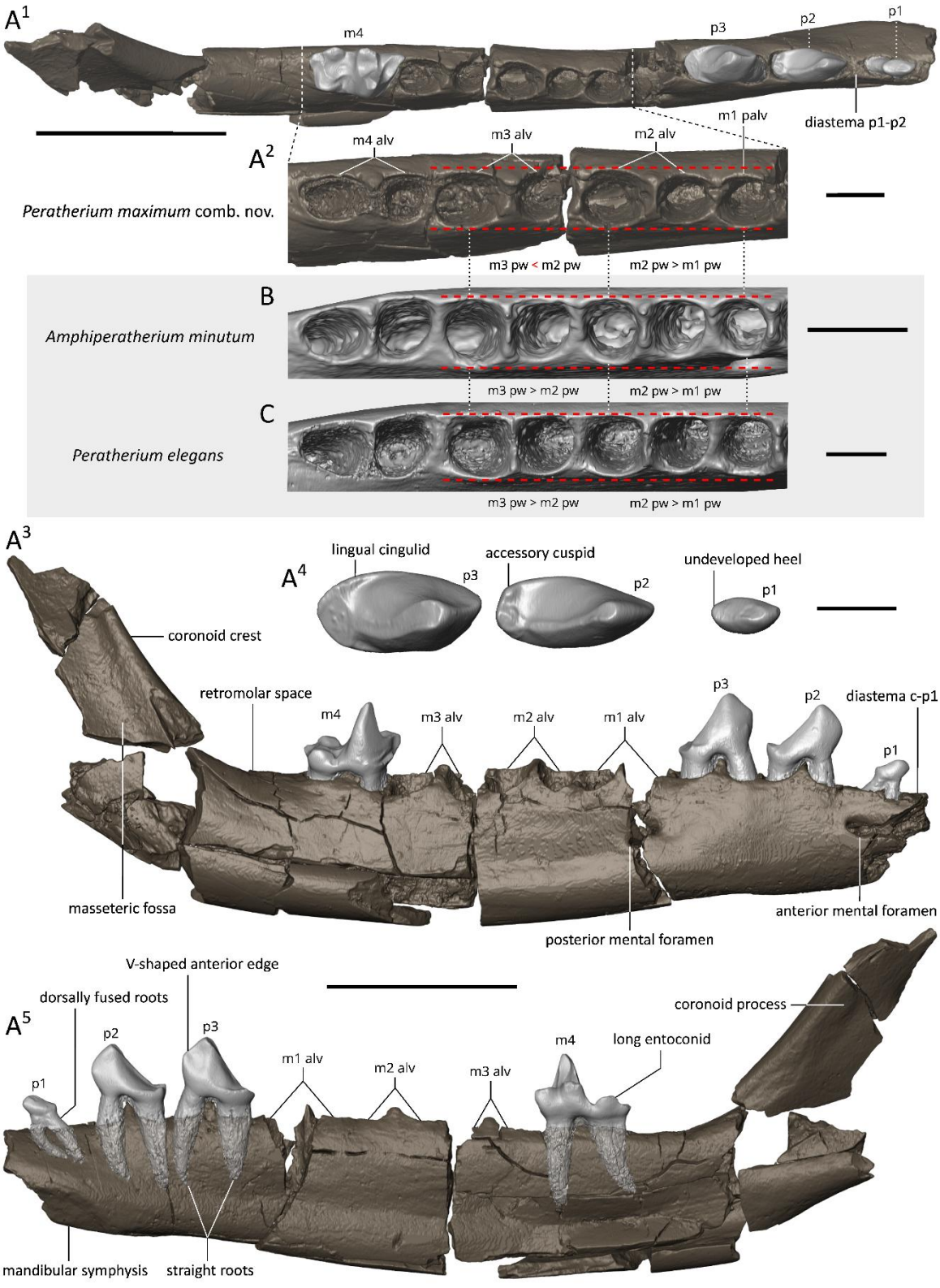


**Figure 6.** Right hemi-mandible fragment with p1-p3, alveoli of m1-m3, and m4 (UM-BRI-17) of *Peratherium maximum* comb. nov., from La Borie (~MP8+9; southern France, Lauragais) ($A^1$-$A^5$) compared with selected late Eocene – Oligocene representatives of *Amphiperatherium* and *Peratherium* (B-C, grey boxes). A. 3D surface model of UM-BRI-17 in occlusal (dorsal) view ($A^1$), with a close-up on m1 to m4 alveoli (with m4 removed) in

occlusal view ($A^2$), in labial (lateral) view ($A^3$), with a close-up on p1-p3 in occlusal view ($A^4$) and in lingual (medial) view, with the roots of the preserved cheek teeth superimposed ($A^5$). B. Reversed occlusal view of the alveoli of m1 to m4 (molars removed) of a 3D surface model of the left hemi-mandible UM-SNB-508, *Amphiperatherium minutum* (Aymard, 1846), from Sainte-Néboule (Quercy; late Eocene, MP18). C. Reversed occlusal view of the alveoli of m1 to m4 (molars removed) of a 3D surface model of UM-VBO-128, *Pt. elegans* (Aymard, 1846), from Valbro (Quercy; early Oligocene, MP22). The red parallel dotted lines ($A^2$, B, C) are positioned on the lingual and labial margins of the largest alveolus of each dentary (posterior alveolus of m2 for *Pt. maximum* comb. nov.; posterior alveolus of m3 for *A. minutum* and *Pt. elegans*). Scale bars: $A^1$., $A^3$., $A^5$., 5 mm; $A^2$., $A^4$., B., C., 1 mm. Abbreviations: alv, alveoli; palv, posterior alveolus; pw, posterior alveolus width.

***Remark on generic attribution***

The former inclusion of the species '*A.*' *maximum* in the genus *Amphiperatherium* is challenged in this study. It is tentatively included in *Peratherium*. This point is developed in discussion.

***Holotype***

MNHN.F.CB198, right M3 (Figure 4Q; Crochet 1979: fig. 7, 1980: fig. 108; L = 2.53 mm, W = 2.91 mm).

***Type locality***

Condé-en-Brie (Paris Basin, Aisne); middle early Eocene (~MP8+9).

***Referred material and measurements***

Material from Pourcy (MP7-MP8+9 interval; PE III biozone): left M1 (MNHN.F.PY18001, L = 2.6 mm, W = 2.66 mm), left m2 (MNHN.F.PY18000, L = 2.41 mm, W = 1.56 mm; MNHN.F.PY18002, L = 2.56 mm, W = 1.65 mm). The m2s were probably studied by Crochet (1980: table 14).

Material from La Borie (southern France, Lauragais; ~MP8+9): fragment of right hemi-mandible with p1-p3, alveoli of m1-m3, and m4 (UM-BRI-17) (measurements in Tables 3-4). A 3D surface model of this specimen is available on MorphoMuseuM.

**Comparative description of the hemi-mandible from La Borie**

UM-BRI-17 is the first early Eocene peratheriine specimen with multiple preserved premolars, and the first *Pt. maximum* comb. nov. specimen preserving associated cheek teeth

(Figure 6A). It also first documents the morphology of the lower premolars and of the dentary of this species.

**Table 3**. Measurements of lower cheek teeth of UM-BRI-17, *Peratherium maximum* comb. nov., from La Borie (Lauragais, ~MP8+9). The m4 measurements are compared to observed ranges of m4s of *Pt. maximum* comb. nov. from Condé-en-Brie (N = 8; this study). Abbreviations: CB, Condé-en-Brie; cH, crown height; L, length; OR, observed range; W, width.

| Locus | L (mm) | W (mm) | L/W | cH (mm) |
|---|---|---|---|---|
| p1 | 0.87 | 0.47 | 1.85 | 0.61 |
| p2 | 2.00 | 0.91 | 2.20 | 1.51 |
| p3 | 2.07 | 1.04 | 1.99 | 1.62 |
| m4 | 2.48 | 1.34 | 1.85 | 1.80 |
| OR m4 CB | 2.38-2.72 | 1.25-1.45 | 1.75-1.90 | - |

***Lower molar***

The specific attribution solely lies on the size and morphology of the m4, the unique molar preserved on the specimen. The anterior root of the m4 is dorsoventrally straight, and the ventral end of its posterior root is slightly curved, directed posteroventrally (Figure 6A[5]). The length and width values of the m4 of UM-BRI-17 fit within the observed range obtained for the eight m4s of *Pt. maximum* comb. nov. from Condé-en-Brie (Table 3), and are much higher than those of the only other peratheriine lower molar from La Borie (*Amphiperatherium bourdellense* Crochet, 1979, from 'Saint-Papoul' in Crochet [1980: table 7]). The long crescentiform entoconid (Figure 6A[5]), with sharp pre-entocristid and postentocristid, is characteristic of m4 of *Pt. maximum* comb. nov. (Crochet 1979, p. 372; 1980: fig. 113). The talonid is relatively labiolingually wide for a peratheriine m4 (Figure 6A[1]), a feature also found on the m4s from Condé-en-Brie (e.g., Figure 7J; Crochet 1980: fig. 113). The m4s of *A. bastbergense* are indistinguishable in length and width from the m4 of UM-BRI-17 (Crochet 1980: table 15). The talonid of m4 is labiolingually narrower in *A. bastbergense* (Figure 6A[1] vs Crochet 1980: fig. 118), but m4s of *Pt. maximum* comb. nov. from Condé-en-Brie with a relatively narrow talonid also exist (e.g., MNHN.F.CB4178). However, the entoconid is not crescentiform in *A. bastbergense* m4 (Crochet 1980: fig. 118).

***Lower premolars***

The complete p1 is minute (Figure 6A), its crown being less than half as long and high, and almost half as wide as the crown of the p2 (Table 3). The p1 of '*Amphiperatherium*' aff. *maximum* from Messel (~MP11) seems relatively longer (Kurz and Habersetzer 2004: fig. 7A), but no measurements are available to confirm it. The other peratheriine p1s known are relatively larger (e.g., Crochet 1980: figs. 139, 217, 232; Storch 1993). This applies particularly to p1 of *Pt. elegans* (Crochet 1980: table 33), of *Amphiperatherium frequens* (von Meyer, 1846) (e.g., Prieto and Rummel 2015: fig. 1A) and of *A. fontense* (pers. obs. [KG] of the holotype), based on the relative size of the alveoli for the last two species. The roots of the UM-BRI-17 p1 are fused close to the base of the crown, whereas the roots of the p2 and of the p3 are unfused (Figure 6A[5]). Unlike peradectids, the roots of the lower premolars are straight rather than curved (Gernelle et al. 2024: table 6), with the exception of the anterior root of the p1, which is curved so that its ventral extremity is almost in contact with the ventral extremity of the straight posterior root (Figure 6A[5]). In occlusal view, only the main cuspid and its distal cristid are distinct on the p1, there is no developed distal heel cuspid, unlike on the p2 and the p3 (Figure 6A[4]). The p1 and the p2 are more procumbent than the p3, because their respective mesial edge is positioned more dorsomesially to the ventralmost point of the anterior root (Figure 6A[3], A[5]). The p3 crown (when not tilted backwards, see below) is as weakly procumbent as on the p3 of *Pt. constans* (Ladevèze et al. 2012: fig. 3Db) and of *A. minutum* (see discussion). In labial and lingual view, the mesial edge of each lower premolar, especially of the p1 and of the p3, is V-shaped (Figure 6A[3], A[5]). The p1 and the p2 are separated by a short diastema (L = 0.65 mm), which is slightly longer than the diastema between the lower canine and the p1. The p1-p2 diastema in '*Amphiperatherium*' aff. *maximum* from Geiseltal-Untere Mittelkohle (Germany, MP12) is almost three times longer than on UM-BRI-17 according to the measurements of Storch and Haubold (1989, p. 98). An inter-alveolar septum, instead of a diastema, separates the posterior root of the p2 from the anterior root of the p3 (Figure 6A[1]). The p3 is higher than the p2 (Figure 6A[3], A[5]; Table 3). The premolars are relatively long, especially the p2, which is more than two times longer than wide (Table 3), but it is not blade-like *sensu* Muizon and Ladevèze (2022, p. 611). Two cuspids are present on the distal edge of the heel of the p2 (Figure 6A[4]). The larger one is connected to the distal cristid of the main cuspid. The smaller adorns the distolingual cingulid, which connects the two heel cuspids (Figure 6A[4]). Such accessory heel cuspids sometimes occur in other peratheriines (e.g., Hooker 2010: fig. 8n-p) and in peradectids (Gernelle et al. 2024: fig. 6a). The heel of the p3 is worn. The lingual cingulid of the p3 is more developed

than that of the p2 (Figure 6A[4]). In occlusal view, the mesial edge of the p2 is straight, whereas the mesial edge of the p3 is curved mesially (Figure 6A[4]).

***Dentary***

Compared to the p1 and the p2, the p3 (when considering both the crown and the roots) is tilted backwards compared to the anteroposterior axis of the dentary (Figure 6A[5]). The retromolar space is slightly shorter than the mesiodistal length of the m4. These two characters indicate

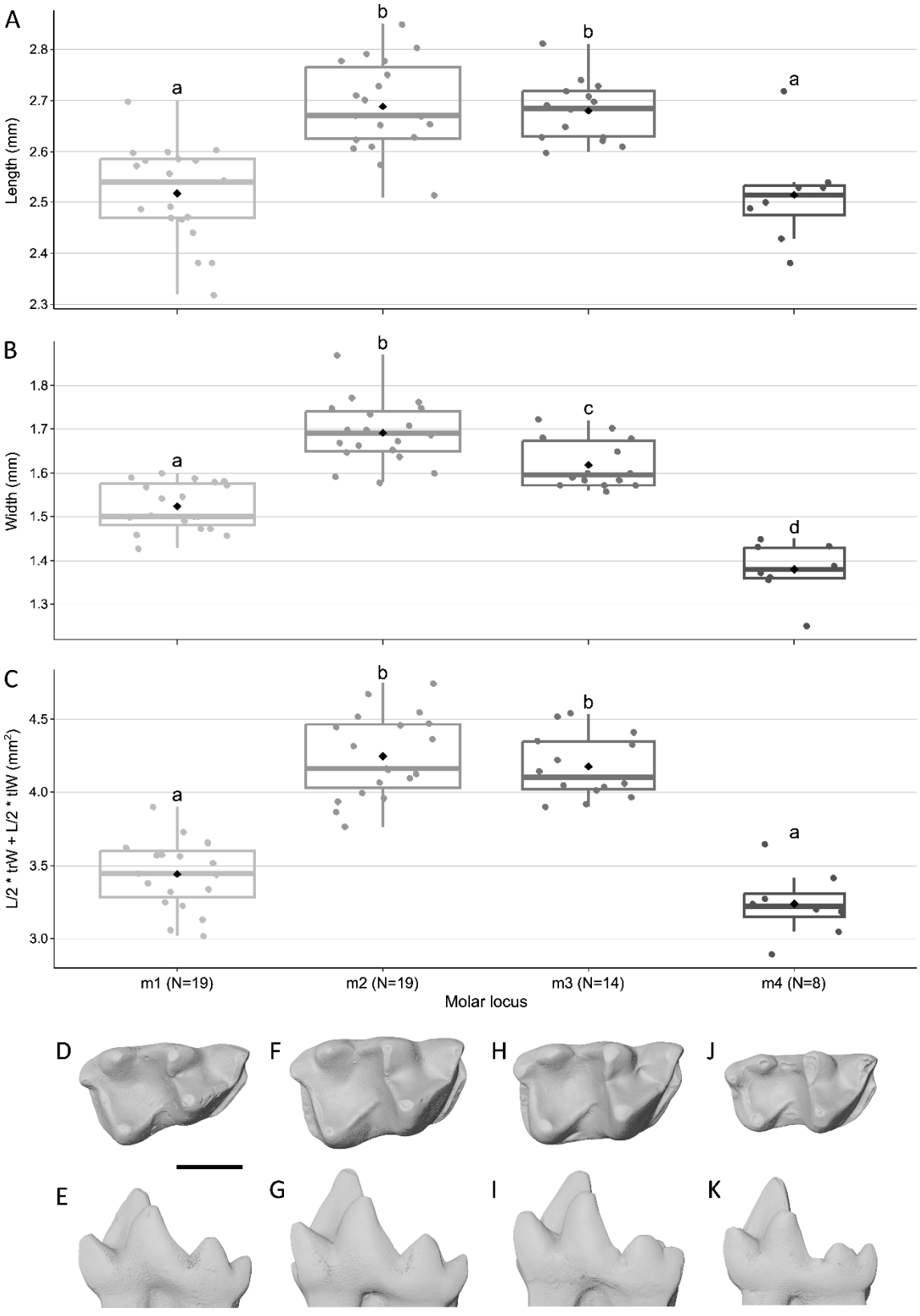


**Figure 7.** A-C. Boxplots of length (A), width (B) and estimated surface area (L/2*trW+L/2*tlW) (C) of isolated m1s, m2s, m3s and m4s of *Peratherium maximum* comb. nov. from Condé-en-Brie (~MP8+9, Paris Basin). The lower molar loci mean values that statistically significantly differ (Games-Howell tests, $P < 0.05$; see main text) are signalled by

a difference in the letter (‘a’ to ‘d’) above each box. Detailed measurements or calculated values are available in Supplemental material 2. D-K. Series of isolated lower molars of *Pt. maximum* comb. nov. from Condé-en-Brie (type locality; ~MP8+9). D-E. MNHN.F.CB2933, right m1 in occlusal (D) and lingual (E) views. F-G. MNHN.F.CB3421, right m2 in occlusal (F) and lingual (G) views. H-I. MNHN.F.CB4977, left m3 in occlusal (H) and lingual (I) reversed views. J-K. MNHN.F.CB820, left m4 in occlusal (J) and lingual (K) reversed views. Scale bar equals 1 mm. Abbreviations: L, length; N, numbers of specimens by group; trW, trigonid width; tlW, talonid width.

that UM-BRI-17 probably belonged to a relatively aged peratheriine individual (see Crochet 1980, p. 35, fig. 5). The ramus mandibularis is partially preserved, represented by fragments of the masseteric fossa and coronoid process, and the dorsal part of the coronoid crest (Figure 6A[3], A[5]). The corpus mandibularis is slender; it is transversely damaged at the level of the anterior root of the m1, and at the level of the anterior root of the m3; its ventral margin is slightly convex. Two mental foramina are present. The anterior one is positioned ventrally to the posterior alveolus of the p1, and the dorsal one is ventral to the anterior alveolus of the m1 (Figure 6A[3]). The deepest point of the dentary is located between below the posterior alveolus of the m2, and below the anterior alveolus of the m3 (h = 4.10 mm; Figure 6A[5]), resembling the condition found in, for example, some pucadelphyids (Muizon and Ladevèze 2022, p. 629). The dentary is only slightly shallower below alveoli of the m4, and is distinctly shallower below alveoli of the premolars (h = 3.05 mm below p2). The posterior extremity of the unfused and shallow mandibular symphysis is preserved. It extends posteriorly to a point approximately ventral to the anterior root of the p2 (Figure 6A[5]). The mandibular symphysis terminates more posteriorly, below the interalveolar septum of the p2, below the posterior root of the p2, or below the anterior root of the p3, in younger peratheriine species for which the symphysis is illustrated (see also Horovitz et al. 2008, p. 133), namely *Amphiperatherium exile* (Gervais, 1848-1852) (Crochet 1980: fig. 140), *Peratherium elegans* (Crochet 1980: fig. 207c), *Peratherium perrierense* Crochet, 1979 (Crochet 1980: fig. 232c), and *Pt. africanum* (Simons and Bown 1984: fig. 2A). The dentary is thicker at the level of the dorsal margin of the symphysis. In medial view, a faint groove extends from a point below the posterior root of the p3 to posteriorly to the m4 (Figure 6A[5]; the junction between the corpus and ramus mandibularis is fragmentary), and as such resembles the mylohyoid groove of the pucadelphyid *Incadelphys* Marshall & Muizon, 1988 (Muizon and Ladevèze 2022: p. 630, fig. 10C-D).

**Table 4**. Measurements (in mm) of lower molar alveoli of UM-BRI-17, *Peratherium maximum* comb. nov., from La Borie (Lauragais, ~MP8+9), compared to those of UM-SNB-508, *Amphiperatherium minutum* (Aymard, 1846), from Sainte-Néboule (Quercy; late Eocene, MP18), and of UM-VBO-128, *Peratherium elegans* (Aymard, 1846), from Valbro (Quercy; early Oligocene, MP22). The greatest length and width values for the posterior alveoli of each specimen are in bold. Abbreviations: A, anterior; alv, alveolus; L, maximum length; P, posterior; W, maximum width.

| Specimen | m1 | | m2 | | | | m3 | | | | m4 | | | |
|---|---|---|---|---|---|---|---|---|---|---|---|---|---|---|
| | P alv | | A alv | | P alv | | A alv | | P alv | | A alv | | P alv | |
| | L | W | L | W | L | W | L | W | L | W | L | W | L | W |
| UM-BRI-17 | 1.15 | 0.84 | 1.01 | 0.80 | **1.27** | **0.95** | - | 0.82 | 1.25 | 0.90 | 0.88 | 0.82 | 1.22 | 0.75 |
| UM-SNB-508 | 0.51 | 0.51 | 0.55 | 0.53 | 0.58 | 0.60 | 0.58 | 0.59 | 0.63 | **0.63** | 0.55 | 0.59 | **0.66** | 0.52 |
| UM-VBO-128 | 0.86 | 0.83 | 0.96 | 0.86 | 0.98 | 0.98 | 0.96 | 0.88 | 1.04 | **1.01** | 0.99 | 1.03 | **1.12** | 0.87 |

***Lower molar alveoli***

In peratheriines, the posterior alveoli of m1 to m3 are labiolingually wider than the respective anterior alveoli (Table 4). The posterior alveolus of the m2 is the widest lower molar alveolus of UM-BRI-17 (Figure 6A$^2$). The width values of the posterior alveolus of lower molars are ordered as follows for this specimen: pw m2 > m3 > m1 > m4 (Table 4). In *Pt. macgrewi*, Bown, 1979, among the earliest herpetotheriines, the posterior alveolus of the m2 is also the widest molar posterior alveolus, based on an edentulous dentary (Beard and Dawson 2009: fig. 5). In the specimens of *A. minutum* and *Pt. elegans* studied here, the posterior alveolus of the m3 is the widest (Figure 6B-C), and the corresponding width values for the molar rows are ordered as follows: pw m3 > m2 > m4 ≥ m1 (Table 4). On UM-BRI-17, the posterior alveoli of the m2 and the m3 are similar in length, whereas that of the m3 is longer on UM-SNB-508 and UM-VBO-128 (Table 4). The longest posterior alveolus is that of the m2 on UM-BRI-17, and that of the m4 on UM-SNB-508 and UM-VBO-128 (Table 4). The alveoli of lower molars of *Pt. maximum* comb. nov. have a relatively mesiodistally elongated, oval aspect (Figure 6A$^2$), the length of each alveolus (except the anterior alveolus of the m4) being much greater than their respective labiolingual widths (Table 4). In contrast, the alveoli of UM-SNB-508 (*A. minutum*) and of UM-VBO-128 (*Pt. elegans*) are round (Figure 6B-C); their length and width measurements are subequal, except for the posterior alveolus of the m4 of UM-SNB-508, and the anterior alveolus of the m2 and posterior alveolus of the m4 of UM-VBO-128, for which L - W ≥ 0.10 mm (Table 4). The total length of the m2 alveoli of UM-BRI-17 is 2.32 mm, hence longer than its m4 alveoli (2.22 mm). Comparatively, the total

length value of the m2 alveoli of '*Amphiperatherium*' aff. *maximum* from Geiseltal-Untere Mittelkohle (MP12) is slightly lower than the one of its m4 alveoli (Storch and Haubold 1989, p. 98), which corresponds to an m2 shorter or as long as the m4. Based on available X-ray illustrations, the m2 of '*Amphiperatherium*' aff. *maximum* from Messel seems also shorter than its m4, unlike *Pt. maximum* comb. nov. from La Borie (Kurz and Habersetzer 2004: fig. 7D).

## Results

### Comparisons of upper molar length and width measurement ratios between selected early peratheriine species

Stylar shelf to talon length ratio values (sL/tL; Table 5) show considerable overlap between *Pt. constans* and *Pt. maximum* comb. nov. for M3. Corresponding values for *Pt. musivum* sp. nov. fit within the observed ranges (OR) of the last two species. The sL/tL values of M2 and M3 of *Pt. maximum* comb. nov. are comparable in OR and mean, whereas the talon of M3 is somewhat longer, relatively to the stylar shelf and on average, than M2 talon in *Pt. constans* (Welch's *t*-test; t = 2.80, d.f. = 12.51, P = 0.016).

**Table 5**. Comparison of stylar shelf length to talon length, stylar shelf length to protocone length, and talonid length to protocone length ratios, between *Peratherium musivum* sp. nov. and samples of *Peratherium constans* Teilhard de Chardin, 1927, and *Pt. maximum* comb. nov. from Condé-en-Brie (~MP8+9), for M2 and M3. Detailed values of calculated ratios are presented in Supplemental material 1. Abbreviations: N, number of specimens; OR, observed range; pL, protocone length; sL; stylar shelf length; tL, talon length.

| Locus | Species | N | sL/tL | | sL/pL | | tL/pL | |
|---|---|---|---|---|---|---|---|---|
| | | | OR | Mean | OR | Mean | OR | Mean |
| M2 | *Pt. constans* | 8 | 1.61-1.85 | 1.73 | 2.15-2.90 | 2.52 | 1.28-1.62 | 1.46 |
| | *Pt. musivum* sp. nov. | 1 | - | - | - | - | 1.33 | - |
| | *Pt. maximum* comb. nov. | 9 | 1.53-1.71 | 1.64 | 1.83-2.25 | 2.03 | 1.15-1.32 | 1.24 |
| M3 | *Pt. constans* | 7 | 1.49-1.72 | 1.60 | 2.26-2.79 | 2.44 | 1.38-1.65 | 1.53 |
| | *Pt. musivum* sp. nov. | 2 | 1.60-1.64 | - | 2.13-2.21 | - | 1.34-1.35 | - |
| | *Pt. maximum* comb. nov. | 9 | 1.56-1.75 | 1.64 | 1.97-2.87 | 2.25 | 1.26-1.64 | 1.37 |

As for stylar shelf to protocone length ratio values (sL/pL; Table 5), the OR of M3 of *Pt. constans* is included in the one of M3 of *Pt. maximum* comb. nov.; the mean value of *Pt. constans* being higher (although fewer specimens are known). The sL/pL values of M3 of *Pt.*

*musivum* sp. nov. are slightly lower than the corresponding (i) mean of *Pt. maximum* comb. nov. (but are included in its OR) and (ii) any values of *Pt. constans*; a similar pattern is recovered for talon to protocone length values (tL/pL), but those of *Pt. musivum* sp. nov. are slightly closer to the mean value of *Pt. maximum* comb. nov. (Table 5). The sL/pL values significantly differ between (i) M2 of *Pt. constans* and of *Pt. maximum* comb. nov. (Welch's *t*-test; t = 4.53, d.f. = 9.97, P = 0.001), M2 of the latter having a longer protocone relatively to the stylar shelf; and (ii) M2 and M3 of *Pt. maximum* comb. nov. (Welch's *t*-test; t = 2.21, d.f. = 11.78, P = 0.048), M2 also having a relatively longer protocone than M3 in this species.

As for talon to protocone length values (tL/pL; Table 5), the same two conclusions regarding the length of the protocone of *Pt. maximum* comb. nov. (here relatively to the talon length) are drawn (Welch's *t*-tests; t = 4.75, d.f. = 9.29, P = 0.001 for M2 of *Pt. constans* vs *Pt. maximum* comb. nov.; t = 3.07, d.f. = 10.95, P = 0.011 for M2 vs M3 of *Pt. maximum* comb. nov.); thus the protocone of M2 of *Pt. maximum* comb. nov. appears relatively longer than that of its M3 and *Pt. constans* M2. Such a difference of relative protocone length between M2 and M3 is not recovered in *Pt. musivum* sp. nov., based on the three known specimens (Table 5), and in *Pt. constans* (e.g., for tL/pL: Welch's *t*-test; t = -1.39, d.f. = 12.89, P = 0.187). Finally, mean tL/pL values also significantly differ between M3 of *Pt. constans* and *Pt. maximum* comb. nov. (Welch's *t*-test; t = 3.06, d.f. = 13.98, P = 0.009). The single tL/pL value available for M2 of *Pt. musivum* sp. nov. is between the lowest corresponding values of *Pt. constans* M2, and the highest value of *Pt. maximum* comb. nov. M2, which slightly overlap.

Based on talon to protocone width values (tW/pW; Table 6), *Peratherium maximum* comb. nov. upper molars have, on average, a significantly relatively wider protocone than those of *Pt. constans* (Welch's *t*-tests; t = 4.30, d.f. = 8.79, P = 0.002 for M2; t = 2.70, d.f. = 10.75, P = 0.021 for M3), with almost no overlap between M2 ratio values of the two species. A Welch's *t*-test yielded no significant difference in tW/pW values between M2 and M3 of *Pt. maximum* comb. nov. (t = -2.15, d.f. = 12.14, P = 0.052). However, because width ratio values are not normally distributed for M2 (Shapiro-Wilk normality test; W = 0.79, P = 0.018), it is noteworthy that a significant difference is recovered with a non-parametric test (Wilcoxon-Mann-Whitney test; W = 14, P = 0.034) instead. The tW/pW values of M2 and M3 of *Pt. constans* do not differ, and those of *Pt. musivum* sp. nov. fit within the OR of respective loci of *Pt. maximum* comb. nov., but not within those of *Pt. constans* (Table 6), as for ratios involving the length of the protocone of M3 (Table 5).

**Table 6**. Comparison of talon width to protocone width ratios, between *Peratherium musivum* sp. nov. and samples (also studied in Table 5) of *Peratherium constans* Teilhard de Chardin, 1927, and *Pt. maximum* comb. nov. from Condé-en-Brie (~MP8+9), for M2 and M3. Detailed values of the calculated ratios are presented in Supplemental material 1. Abbreviations: N, number of specimens; OR, observed range; pW, protocone width; tW, talon width.

| Locus | Species | N | tW/pW | |
|---|---|---|---|---|
| | | | OR | Mean |
| M2 | *Pt. constans* | 7 | 1.92-2.52 | 2.14 |
| | *Pt. musivum* sp. nov. | 1 | 1.85 | - |
| | *Pt. maximum* comb. nov. | 9 | 1.59-1.92 | 1.70 |
| M3 | *Pt. constans* | 7 | 1.88-2.58 | 2.22 |
| | *Pt. musivum* sp. nov. | 2 | 1.69-1.84 | - |
| | *Pt. maximum* comb. nov. | 8 | 1.63-2.28 | 1.88 |

**Quantitative analysis based on isolated lower molars of *Peratherium maximum* comb. nov.**

The m2s and m3s of *Pt. maximum* comb. nov. from Condé-en-Brie do not significantly differ in mesiodistal length (Supplemental material 3: Figure S1) or estimated surface area (Supplemental material 3: Figure S4), so do m1 and m4 for these variables (Figure 7A, C; Supplemental material 3). The m2 and m3 are significantly longer and have a larger surface area than m1 and m4. The m1 and m4 overlap m2 and m3 in length; this overlap is lesser for the estimated surface area (even absent between m4 and m2-m3; Figure 7C). All molar loci differ significantly from one another in width (Supplemental material 3: Figure S2) and talonid width (Supplemental material 3: Figure S3). Isolated m2s are the widest based on mean values (Figure 7B). The mean width and talonid width values are ordered as follows for isolated lower molars: m2 > m3 > m1 > m4 (Figure 7B; Supplemental material 3: Figure S6A); a relationship identical to that recovered based on the molar posterior alveoli of UM-BRI-17 (see above; Table 4). Furthermore, it is worth mentioning that the relative talonid width (tlWr) values of m2 and m3 significantly differ (Supplemental material 3: Figure S5), tlWr values being higher for m2 on average (Supplemental material 3: Figure S6B).

***Remark***

In *Peratherium maximum* comb. nov., m3s are sometimes difficult to distinguish from m2s or m4s. Here, lower molar loci have been confidently identified using the following characters. From m1 to m4: in occlusal view (Figure 7D, F, H, J), (i) the trigonid becomes labiolingually wider relative to the talonid (and the relative talonid width values becomes significantly lower from m1 to m3; Supplemental material 3: Figure S6B); (ii) the protoconid becomes more transversely aligned with the metaconid; (iii) the hypoflexid widens somewhat labiolingually; and (iv) the distolingual edge of the talonid is less and less curved, and the lingual edge of the hypoconulid labiolingually shortens; in lingual view (Figure 7E, G, I, K), (v) the metaconid becomes relatively shorter mesiodistally and the paraconid becomes relatively taller; (vi) the paraconid – metaconid notch becomes open higher relative to the metaconid – entoconid notch; (vii) the entoconid – hypoconulid notch becomes open higher relative to the metaconid – entoconid notch. Finally, (viii) the protoconid is relatively higher on m4; and (ix) the postcingulid is prominent on all molars except m4, on which it is partly developed to completely indistinct (Figure 7J).

## Discussion

### Reappraisal of the specific status of MP7-MP8+9 interval 'larger' peratheriines: phylogenetic, biochronologic, and palaeobiogeographic implications

***Characterisation of* Peratherium musivum *sp. nov. dental morphology***

The specific attributions of herpetotheriid isolated cheek teeth from the early Eocene are primarily based on size (e.g., Smith and Russell 1992; Smith R and Smith T 2004; Beard and Dawson 2009, p. 200; Hooker 2010, p. 17). Similarly, the molars of *Pt. musivum* sp. nov. differ primarily in size (Figure 4O vs Figure 4P vs Figure 4Q), without overlapping, from those of its coeval species, *Pt. constans* and *Pt. matronense*, which are smaller (body mass of ~51-56 g using the length of the M3 of *Pt. musivum* sp. nov. in the appropriate predictive equation of Gordon [2003: fig. 7]; vs ~22 g calculated using the length of the M2 holotype of *Pt. constans* [Ladevèze et al. 2012: fig. 1a] in the appropriate predictive equation), and *Pt. maximum* comb. nov., which is larger (body mass of ~120g, calculated using only the length of the M3 holotype). The matching between isolated lower and upper molars of *Pt. musivum* sp. nov. is thus possible based on the homogeneous size of these elements (e.g., M1 length ≈ m1 length, see Tables 1-2; as in *Pt. maximum* comb. nov., see measurements of

MNHN.F.PY18001 above vs m1 measurements in Supplemental material 2). *Peratherium* sp. indet. 1 in Crochet (1980), in which the holotype of *Pt. musivum* sp. nov. (MNHN.F.SN122) was included, does not form a 'monospecific lineage' (*contra* Crochet 1980: p. 217, fig. 239), and contains representatives of presumably two peratheriine species, as Crochet (1980, p. 214) himself suggested (but these are probably not closely related). A relatively large stylar cusp C is not a similarity between MNHN.F.SN122 and *Pt. maximum* comb. nov., because M3s of the latter have a dominant stylar cusp B (Figure 3A; *contra* Crochet 1980, p. 233). The few relevant morphological differences (i.e., the least subjected to intraspecific variation) between molars of *Pt. constans*, *Pt. musivum* sp. nov. and *Pt. maximum* comb. nov. are subtle (see diagnosis of *Pt. musivum* sp. nov.) and mainly concern the distolingual talonid cuspids of the lower molars, and the stylar height relationships and the outline of the upper molars. More specifically, we hypothesise that *Pt. musivum* sp. nov. and *Pt. maximum* comb. nov. are close relatives, because they share the stylar cusp D apex more ventral than stylar cusps B and C apices on M1, the lack of distal emargination of the M2 crown in occlusal view, and the lingual edge of the hypoconulid longer than its labial edge on m1. Formal phylogenetic analyses will be required to test this hypothesised relationship.

The analysis of the three types of ratios calculated using length measurements (Table 5) revealed that shape differences between upper molars of the studied species mainly occur at the level of the protocone, rather than the stylar shelf or the whole talon. According to Godinot (1981, p. 55), (i) the lingual base of the protocone of the M2 MNHN.F.RI220 is less rounded than in M2 of *Pt. maximum* comb. nov., and (ii) the trigonid of the m2 MNHN.F.RI368 is longer than its talonid, whereas the reverse could be true for most lower molars of *Pt. maximum* comb. nov. The latter statement seems difficult to assess, at first, based on the few m2s of *Pt. musivum* sp. nov. and of *Pt. maximum* comb. nov. here illustrated (Figure 5D vs Figures 5P, 7F). If it is true, either the trigonid itself could have become mesiodistally shorter in *Pt. maximum* comb. nov., or the talonid could have become longer. The mesiodistal length of the talonid must be correlated with the length of the protocone, because there is a functional relationship between these structures during molar occlusion (e.g., Johanson 1996, p. 1028 and references therein). The direct comparison of the relative protocone length of M2 of *Pt. musivum* sp. nov. is of limited value here, because, although *Pt. maximum* comb. nov. has a relatively longer M2 protocone than *Pt. constans* on average, the only M2 specimen of *Pt. musivum* sp. nov. does not permit to conclude regarding this locus in this species. However, based on a few specimens, we detected (i) that the relative protocone

length of M3 and the relative protocone width of M2 and M3 of *Pt. musivum* sp. nov. are closer to those of *Pt. maximum* comb. nov. (Tables 5-6), and (ii) a change in the relative length of the protocone between M2 and M3 in *Pt. maximum* comb. nov., the protocone of M2 (and thus the talonid basin of m2) being relatively longer on average, whereas such a difference has not been noted between these loci in both *Pt. constans* and *Pt. musivum* sp. nov. Thus, *Pt. musivum* sp. nov. (i) possibly exhibits a slight relative enlargement of the protocone/talonid compared to *Pt. constans*, and (ii) possibly lacks the relative enlargement of the protocone/talonid of its second molars compared to its third molars contrary to *Pt. maximum* comb. nov., although more specimens of *Pt. musivum* sp. nov. will be crucial to characterise with more confidence such slight shape differences between isolated molars.

***Biochronologic and palaeobiogeographic considerations***

*Peratherium musivum* sp. nov. is herein recorded in Le Clot, where it is coeval with the small *Pt. constans* (Table 7; Figure 5K-M vs Figure 5N; Marandat et al. 2012, p. 428), a conclusion founded on a few, mostly fragmentary cheek teeth (N = 2 out of 10 metatherian specimens). Thus, given the age of Le Clot (see Materials and methods section), peratheriines much larger than *Pt. constans* definitely first occur between the PETM and the ETM2, approximately 1 myr after the appearance of this subfamily in the fossil record of Europe. Perhaps unexpectedly, no metatherian species larger than *Pt. constans* or *Peradectes crocheti* Gernelle, 2024, are recorded from the better sampled (for small mammals) Palette (in Provence; N > 40 metatherian specimens) and Fordones (N > 60 metatherian specimens) localities, which have been correlated in age with Le Clot based on the exclusive shared occurrences of the two louisinid condylarths *Lessnessina praecipuus* (Russell, 1987) and *Paschatherium plaziati* Marandat, 1989, with Palette, and *Pa. plaziati* in addition to the ischyromyiform rodent *Corbarimys hottingeri* Marandat, 1989, with Fordones (Godinot et al. 1987; Marandat 1991; Marandat et al. 2012; Gernelle et al. 2024: table 1). It should be noted that an undescribed rare second rodent species markedly larger than *C. hottingeri* occurs in Le Clot, the same pattern for Palette, with an undescribed rare species larger than the common *C. cezannei* (Hartenberger, 1987) (Marandat et al. 2012, p. 427). The occurrences of *Pt. musivum* sp. nov. and of *Peradectes crocheti*, restricted to the MP7-MP8+9 interval (this study; Gernelle et al. 2024), further highlight the weak resolution of the Ypresian MP reference levels, as currently defined (see BiochroM'97 1997), when it comes to describe evolutionary dynamics of European metatherians. Moreover, the presence of *Pt. musivum* sp. nov. and of *Peradectes crocheti* in mammal faunas older and younger than the ETM2 (this study;

Gernelle et al. 2024) strengthens conclusions stating that this hyperthermal event could be unassociated with a significant faunal turnover (Abels et al. 2012), at least in Western Europe (Noiret et al. 2016, p. 478). *Peratherium musivum* sp. nov. is recorded simulteanously in localities from both northern (Soissons, Pourcy, and possibly Abbey Wood) and southern France (Le Clot, Fournes, Rians), which reinforces the absence of apparent biotic provincialism in European metatherians, as proposed in recent studies (Gernelle et al. 2024; Wessels et al. 2024). Unsurprisingly, the absence of provincialism in larger early peratheriine species newly extends to ~MP8+9 mammal faunas, because *Peratherium maximum* comb. nov. is herein recorded in La Borie. At this time, the northern/southern provincialism pattern characteristic of most components of the MP7-MP8+9 interval Eutherian faunas from Western Europe attenuates (e.g., Solé et al. 2014: fig. 11, 2018: fig. 18).

| | Peratheriine taxon | MP7 | MP7-MP8+9 time interval | | | | | | |
|---|---|---|---|---|---|---|---|---|---|
| | | PE I | PE II | | | PE III | | | |
| | | Do | *Clo* | Sn | Me | Aw | *Frn* | *Ri* | Py |
| Before this study | *Pt. constans** or ***Pt. matronense*** | x* | *x** | | **cf.** | | ***cf.*** | ***x*** | |
| | *Pt.* sp. 1 in Crochet (1980) | | | x | | | | | |
| | *Amphiperatherium maximum* | | | cf. | x | | *cf.* | *cf.* | x |
| | *A.* sp. 2 in Hooker (2010) | | | | | x | | | |
| | *Amphiperatherium goethei* | | | | | | | *x* | |

**Table 7**. Occurrences of peratheriine taxa in MP7 to MP7-MP8+9 interval localities, both before and in the present study. Southern France localities and associated occurrences are in italics. Among localities in or correlated with the PE II biozone, only Le Clot is demonstrated to be anterior to the ETM2. Note that the hardly distinguishable *Peratherium constans* Teilhard de Chardin, 1927 (*), and *Peratherium matronense* Crochet, 1979 (bold occurrences) remain unreviewed (see Ladevèze et al. 2012, p. 257). Abbreviations for localities: Aw, Abbey Wood; Clo, Le Clot; Do, Dormaal; Frn, Fournes; Me, Meudon; Py, Pourcy; Ri, Rians; Sn, Soissons.

| | | | | | | | | | | |
|---|---|---|---|---|---|---|---|---|---|---|
| This study | *Pt. constans** or ***Pt. matronense*** | x* | *x** | | **cf.** | | ***cf.*** | ***x*** | |
| | *Peratherium musivum* sp. nov. | | *x* | x | | cf. | *x* | *x* | x |
| | *Peratherium maximum* comb. nov. | | | | | | | | x |

The lower molar MNHN.F.RI385 (Figure 5H) was first attributed to m1 or m2 of *Amphiperatherium goethei* Crochet, 1979 (Godinot 1981, p. 54). It is actually an m1 given the low labiolingual width value of the trigonid compared to the talonid. MNHN.F.RI385 is labiolingually wider and has a more distally projecting hypoconulid (i.e., with a strongly curved postcristid) than m1 of *A. goethei* from its type locality, Bouxwiller (~MP13; Crochet 1980: table 12, fig. 95). Regarding these characters, MNHN.F.RI385 is similar to the m1 MNHN.F.SN2507 and is here allocated to *Pt. musivum* sp. nov. As a result, *A. goethei* becomes absent from Rians and from the whole MP7-MP8+9 interval (Table 7), the oldest occurrence of the species now being from Avenay (MP8+9; Crochet 1980, p. 89). '*Amphiperatherium*' *maximum* was listed in the Meudon fauna (MP7-MP8+9 interval, PE II; Russell et al. 1988). Among the metatherian material from this locality, a single trigonid fragment preserving only complete protoconid and metaconid (MNHN.F.ME15976) is markedly larger, similar to what is expected for a specimen of '*A.*' *maximum*. However, its protoconid and metaconid are subequal in height, which is a character unknown in Laurasian metatherians, but often present in eutherians (see Gernelle et al. 2024, p. 38). Relatively large herpetotheriid species are thus absent from Meudon (Table 7). The earliest occurrence of *Pt. maximum* comb. nov., a species typical of the MP8+9 and ~MP8+9, is now from the Pourcy fauna (Crochet 1980: table 14; this study), where it is newly coeval with *Pt. musivum* sp. nov. (Table 7), which is recorded only in part of the MP7-MP8+9 interval. This unique co-occurrence suggests that the mammal fauna of Pourcy, if homogeneous, could be intermediate in age between Fournes/Rians and Mutigny (the oldest locality younger than MP8+9).

*Peratherium musivum* sp. nov. spans approximately between 1 and 2 myr (depending on the age of the Pourcy fauna) of the fossil record of the early Eocene, during the MP7-MP8+9 interval (at least ~55-54 Ma based on the respective age of Le Clot and Fournes). The older faunas of Dormaal (MP7), and Silveirinha (Portugal) and Le Quesnoy (Paris Basin) (both ~MP7) solely yielded smaller herpetotheriids (Nel et al. 1999; Estravís 2000; Ladevèze et al. 2012; pers. obs. [KG] of Le Quesnoy metatherians), and *Pt. musivum* sp. nov. is also absent from the well-sampled faunas of the MP8+9 and ~MP8+9 localities of the Paris Basin, from which herpetotheriids are abundant (Mutigny, Avenay, Condé-en-Brie, Sables de Brasles, Sézanne-Broyes), following the review of the MNHN mammal collection by one of us (KG).

Consequently, among the first ascertained herpetotheriid species, at least some had a relatively short apparent longevity expected for small mammals (e.g., Flynn et al. 1995), including smaller metatherians (e.g., Tarquini et al. 2022: fig. 2), like European peradectids (Gernelle et al. 2024: fig. 16). Such a finding is in line with the median and mean longevity values known for Cenozoic mammal species (e.g., Marshall 2017), and contrasts with the long apparent duration of various Eocene Laurasian mammal species (e.g., Dunn and Townsend 2019, p. 12), such as most Eocene herpetotheriine species (pending further revision) recorded as early as the early Eocene (Krishtalka and Stucky 1983b: fig. 7; Murphey et al. 2018, ~12.4 myr duration for *Herpetotherium marsupium* Troxell, 1923), and unrevised peratheriine species (e.g., *A. bourdellense*; MP8+9 to MP16 reference levels; Figure 1).

## Investigating significant dental characters: is *Amphiperatherium* likely to be represented in the earliest phases of Peratheriinae evolution?

### *History and definitions of* Amphiperatherium *Filhol, 1879, and the* Peratherium *vs* Amphiperatherium *dichotomy: a critical review*

The taxonomy of peratheriines at the generic level is confusing. Below, we report on the lability of the taxonomic content and of the diagnostic characters of *Amphiperatherium*, which varied over time between authors, with respect to those of *Peratherium*. Three taxonomic groups of peratheriines from the Quercy phosphorites were first envisioned by Filhol (1877, p. 468), namely *Peratherium* as a first group, a second group composed of specimens that do not exhibit the characters of *Peratherium* (probably later designated as *Amphiperatherium*), and a third group characterised by only a few features of *Peratherium*. The sub-genus *Amphiperatherium* was later created by Filhol (1879, p. 204) for a new peratheriine species from Saint-Gérand-le-Puy (in Allier, France), of which the mandible displays lower molars that do not increase in volume from the m1 to the m4, and a putatively unusual morphology of the m4 talonid (note that the m4 talonid of metatherians shows recurring intraspecific variation; see Martin 2005: fig. 4). *Amphiperatherium* was subsequently considered by Filhol (1881, pp. 65-68) alternatively as a genus (two times) and a sub-genus (one time). The two diagnostic characters of *Amphiperatherium* then retained, the absence of increase in volume from the m1 to the m4, and the p3 not being the highest of the premolars (following the characters of Aymard [1850, pp. 83-84]; instead of the characters related to the morphology of the m4 talonid, previously defined), still concerned only lower cheek teeth. A peratheriine hemi-mandible preserving m4 was described as intermediate in morphology between *Peratherium* and *Amphiperatherium* by Depéret and Douxami (1902, pp. 78-82), a conclusion

somewhat similar to the early recognition of more than two groups of peratheriines proposed by Filhol (1877). A possible synonymy of the two genera was thus already argued (Depéret and Douxami 1902, p. 79), their typical features, as then defined, presenting intrageneric variation. In the seven decades following the publication of Depéret and Douxami (1902), no new species of *Amphiperatherium* was created (e.g., Simpson 1930, p. 32) and this genus was eventually declared invalid (Koenigswald 1970).

Initiating the exhaustive taxonomic reappraisal of Cenozoic metatherians from Europe, using numerous mandibles from the Quercy phosphorites, Crochet (1969, p. 2041) suggested that *Peratherium* could likely be split in further studies. *Amphiperatherium* was later resurrected by Crochet (1977a), this time with a time range covering the whole evolutionary history of peratheriines (early Eocene to Middle Miocene). The relatively longer posterior lower molars (instead of their relative increase in volume; thereby following Aymard [1850, p. 84]) should be considered as a 'trend' to elongation in *Peratherium*, 'that develops gradually over time', according to Crochet (1977a, p. 357, 1977b, p. 129). Even if exceptions have been noted for this character in approximately half of the *Peratherium* species studied by Crochet (1980) (Simons and Bown 1984, p. 543), its less restrictive definition as a gradual trend with intrageneric variation was sufficient for Crochet (1980) to retain it as a diagnostic feature. Inconsistencies in the specific occurrences of the two states of the character regarding the relative length of posterior lower molars, which contradict the diagnosis of the genus, are also reported in *Amphiperatherium*, due to intraspecific variation in the type species *A. frequens*. In particular, the holotype of *A. frequens* and some mandibles from Saint-Gérand-le-Puy (the material based on which *Amphiperatherium* was erected) have m4 longer than m3 (Koenigswald 1970, pp. 49, 55), which is a trait stated in the diagnosis of *Peratherium* from Crochet (1977a, 1980), provided that the studied sample is large enough (Crochet 1977b). Occasionally, the m3 can also be longer than and as wide as the m2 in *A. frequens* (Koenigswald 1970, p. 55; Prieto and Rummel 2015: fig. 2B) (see also *A. minutum*; e.g., Crochet 1978, p. 234; Wessels et al. 2024: table 2), while the diagnosis of *Amphiperatherium* from Crochet (1977a, 1980) specifies that these molar loci are 'subequal in size' (instead of 'length' or 'volume' of the previous diagnoses) within the genus. Mean values should be used to compare this trait between several species. Altogether, morphological differences between lower molars of *Peratherium* and *Amphiperatherium* remain elusive (see below; Figure 8; Crespo et al. 2022: table 2). Probably partly for these reasons, characters related to the

morphology of the stylar shelf of upper molars were considered more reliable by Crochet (1977a, p. 357), in order to distinguish marsupialiform genera from Europe.

Ten valid peratheriine species were afterwards placed in *Amphiperatherium*, and thirteen valid species in *Peratherium*, not including taxa that are in open nomenclature (Crochet 1979; Simons and Bown 1984; Kurz 2007; Ladevèze et al. 2012). Doubts have been raised regarding the validity of *Amphiperatherium*, based on the characterisation of intraspecific morphological variation in the oldest series of peratheriine dental remains (Ladevèze et al. 2012). Several authors attempted to propose new differential diagnostic characters for peratheriine genera. For example, the entoconid has been described as 'conical' or 'more conical' in *Peratherium* (Kurz 2007, p. 46; Hooker 2010, p. 16), and 'oval-like' (or respectively 'less conical') in *Amphiperatherium* (e.g., Kurz 2007, p. 47). However, figured comparisons of lower molars of *A. minutum* and *Peratherium cuvieri* (Fisher, 1829) (Selva and Ladevèze 2017: fig. 5A vs fig. 5B), and of *A. minutum* and *Pt. elegans* (Figure 8A, C), show that such a discrimination based on overall shapes of the entoconid is impossible. In the same way, the presence of a curved rather than almost straight anterior cristid on the p2 and p3 (Kurz 2007, p. 47), and the procumbency of the p3 (Hooker et al. 2008, p. 642), have been proposed to be diagnostic of

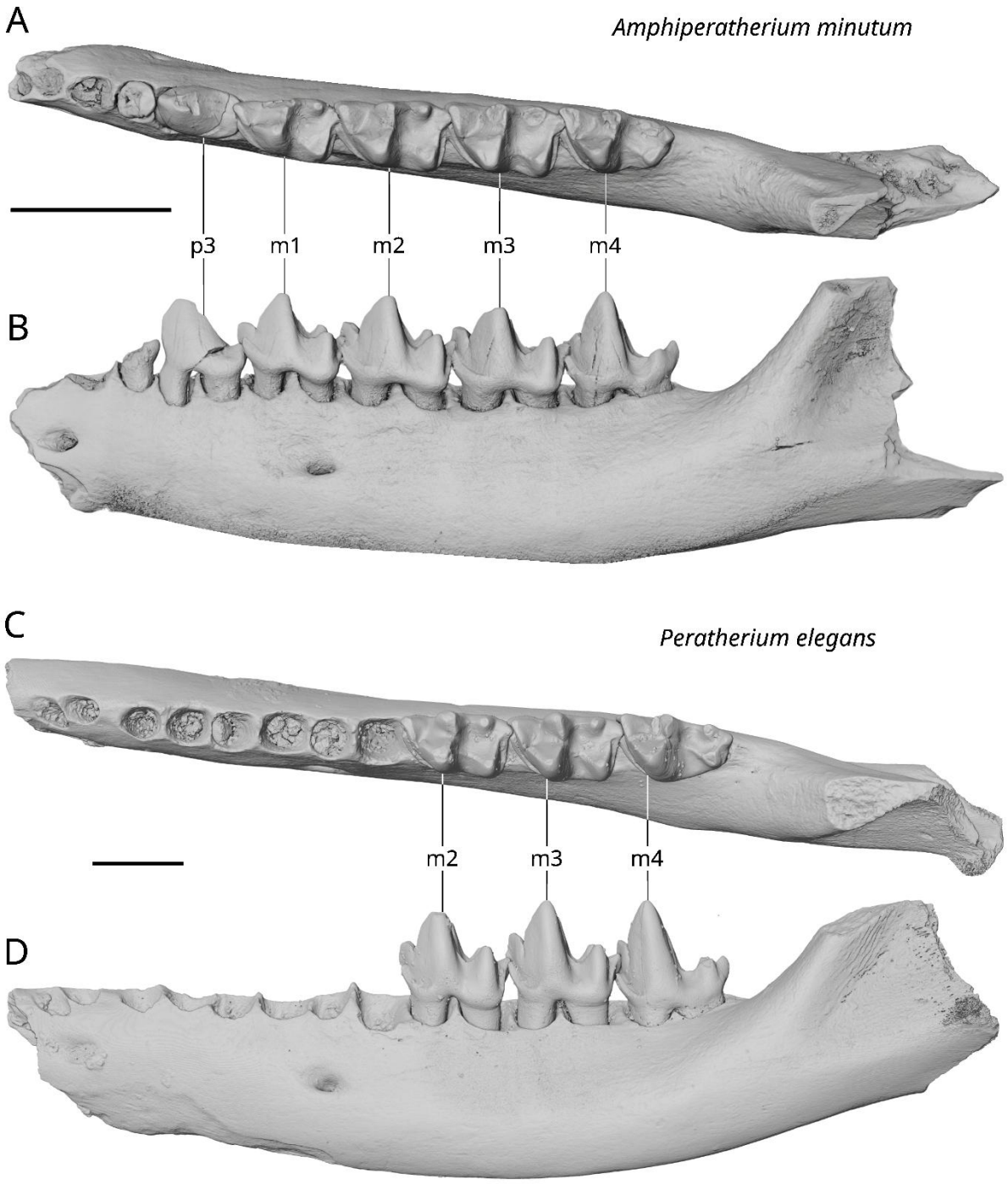


**Figure 8.** Comparison of hemi-mandibles of *Amphiperatherium minutum* (Aymard, 1846) (A-B) and *Peratherium elegans* (Aymard, 1846) (C-D), based on volume renderings. A-B. UM-SNB-508, left hemi-mandible with alveoli of p1-p2, and p3-m4, from Sainte-Néboule (Quercy; late Eocene, MP18) (Crochet 1978: fig. 1D) in occlusal (dorsal) (A), and labial (lateral) (B) views. C-D. UM-VBO-128, left hemi-mandible with alveoli of p1-m1, and m2-m4, from Valbro (Quercy; early Oligocene, MP22) (Crochet 2016: fig. 1F) in occlusal (dorsal) (C), and labial (lateral) (D) views. Scale bars equal 2 mm.

*Amphiperatherium*. Here again, multiple inconsistences exist. '*Amphiperatherium*' aff. *maximum* (Geiseltal-Untere Mittelkohle) has a straight anterior cristid on the p3 (Kurz 2007, p. 33), whereas this cristid is curved on the p2 and the p3 of *Peratherium* aff. *monspeliense* from Geiseltal-Untere/Obere Mittelkohle (Kurz 2007, pp. 30-31), which contradicts the expected generic occurrences of the character states defined by Kurz (2007) herself. Intraspecific and even intra-individual variation probably exist for this character, because the hemi-mandible from La Borie has a p2 with a straight anterior cristid, and a p3 with a curved anterior cristid (Figure 6A[4]). As for the procumbency of the p3, this lower premolar is not procumbent in at least some *A. minutum* specimens (Figure 8B), contrary to the diagnosis. The only undoubted differences between *Peratherium* and *Amphiperatherium* were more recently argued to concern their petrosal anatomy (Ladevèze et al. 2020, p. 13). However, the differences highlighted by Ladevèze et al. (2020) between the two genera possibly reflect interspecific rather than intergeneric morphological variation, because, among *Amphiperatherium*, only the petrosal anatomy of *A. minutum* has been investigated, and compared to that of two species of *Peratherium* (*contra* Ladevèze et al. 2020). Finally, in the same way, the postmetacrista has been described as inconspicuous in *Peratherium*, contrary to the tall distal wall formed by the postmetacrista of *Amphiperatherium* (Ladevèze et al. 2020, p. 14), but the earliest Eocene *Pt. constans* present such a well-developed postmetacrista (e.g., Ladevèze et al. 2012: fig. 4A; pers. obs. [KG] of NMB Om.158, fig. 35 in Crochet 1980).

***Generic status of* Peratherium musivum *sp. nov.***

It was stated that primitive *Peratherium* species from the early Eocene (i.e., *Pt. constans* and *Pt. matronense*) are less easily distinguishable from *Amphiperatherium* (Hooker et al. 2008, p. 643). The generic status of the MP7-MP8+9 interval species *Pt. musivum* sp. nov. also appears blurry when considering the diagnostic differences between *Peratherium* and *Amphiperatherium*, as they are summarised by Hooker et al. (2008, p. 642). In fact, based on this emended differential diagnosis (the most recent for peratheriine genera), the arguments for the tentative generic attribution of *Pt. musivum* sp. nov. are as follows. Five out of the seven characters proposed in the diagnosis can be evaluated for this species, due to unknown p3 and m4. (i) The two m1s and the only ascertained m2 of *Pt. musivum* sp. nov. are smaller than the ascertained m3 allocated to this species (Table 2). Such an apparent enlargement of m3, relatively to m1 and m2, would be evocative of *Peratherium* according to the diagnosis (as for upper molars, complete M1 and M2 are unknown for *Pt. musivum* sp. nov.). However, note that this conclusion is only based on a few isolated lower molars, representing different

individuals from different localities, and that intraspecific variation is known in other species (see above). (ii) As for the relative size of the paracone and metacone mentioned by Hooker et al. (2008), it was demonstrated that strong variation in this trait exists within a comprehensive series of molars for a given herpetotheriid species (Ladevèze et al. 2012: fig. 4Ca vs fig. 5Ga). Thus, this character surely does not differentiate *Peratherium* from *Amphiperatherium*. (iii) Stylar cusp B is smaller than or as high as stylar cusp C in M3 of *Pt. musivum* sp. nov., and stylar cusp B is smaller than stylar cusp D on its M1. Consequently, stylar cusp B is herein considered 'small' (although higher than stylar cusps A and D on M3), which is alike *Amphiperatherium* in the diagnosis. (iv) The paraconule and metaconule of *Pt. musivum* sp. nov. are not significantly relatively larger than those of equivalent molar loci of the smaller *Peratherium* species, as *Pt. constans* (e.g., Figure 4N vs Figure 4P) or *Pt. elegans* (e.g., Ladevèze et al. 2012: fig. 7a-b; Crochet 2016: fig. 1A). (v) Because the strength of the postcingulid was demonstrated to vary in *Pt. elegans* (Ladevèze et al. 2012, p. 260), a purported stronger postcingulid than in *Amphiperatherium* is not a trait of *Peratherium*. Altogether, among the two out of five available characters not proven to represent morphological intraspecific variation (the size of the conules and of stylar cusp B of upper molars), only one (the size of stylar cusp B) would be indicative of *Peratherium* rather than *Amphiperatherium*.

The tentative generic identification here conducted emphasises serious application difficulties of the *Peratherium* vs *Amphiperatherium* dichotomy, when it comes to peratheriine species documented only by isolated molars (e.g., *contra* Crochet in Rémy et al. 1997, p. 715). Furthermore, the holotype M3 of *Pt. musivum* sp. nov. was first attributed to *Peratherium* by Crochet (1980), seemingly because the mesiodistally slender outline of this molar, with a labiolingually wide protocone, vaguely evokes the outline of M3 of *Pt. monspeliense* (Crochet 1980, p. 214), whereas all lower molars of *Pt. musivum* sp. nov. described before this study were included in *Amphiperatherium* (Godinot 1981; Marandat 1991; Louis 1996). Besides size, a few subtle morphological differences distinguish *Pt. musivum* sp. nov. from *Pt. constans* and '*A.*' *maximum* (see above). Due to the lack of relevant applicable definitions of *Peratherium* and *Amphiperatherium*, the provisional allocation of *Pt. musivum* sp. nov. to *Peratherium* (a longevity value on the order of that of *Peratherium* [> 30 myr; see BiochroM'97 1997] is unexpected for small mammal genera [e.g., Hoek Ostende et al. 2023]) thus lies exclusively on the fact that the earliest peratheriine species, *Pt. constans*, belongs to *Peratherium* (Ladevèze et al. 2012), which is the oldest valid peratheriine genus. Due to the

definition of *Pt. musivum* sp. nov., which has relatively small stylar cusp B on M1 and M3, and the fact that '*Amphiperatherium*' *maximum* has clearly dominant stylar cusp B on M3 (Figure 3A), the relative size of stylar cusps (used in the diagnoses of *Peratherium* and *Amphiperatherium*; Crochet 1980; Hooker et al. 2008) are thus also concerned by interspecific variation in peratheriines, alike in Peradectidae (Gernelle et al. 2024: table 3, fig. 14).

***Original dentally-related characters of* Peratherium maximum *comb. nov. and functional implications. Towards a phylogenetic systematics approach of peratheriine's evolutionary history***

The comparisons of the hemi-mandible of *Peratherium maximum* comb. nov. from La Borie and conspecific lower molars from Condé-en-Brie reveal that this early peratheriine presents original morphological characters that differ from younger species of both the genera *Peratherium* and *Amphiperatherium* (but still in part not assessable for *Pt. constans*; Ladevèze et al. 2012), namely: (i) the p1 is minute relatively to the p2 and the p3, more so than in any other peratheriines; (ii) most lower molar alveoli are relatively longer than wide; and (iii) m2 is the widest lower molar locus (*contra* Crochet 1980, p. 98, diagnosis of '*A.*' *maximum* in which m2s and m3s are considered equally wide). As for the latter character, the results of the quantitative analysis performed with the length and width values of isolated lower molars of *Pt. maximum* comb. nov. (Figure 7B) show that measurements of lower molar alveoli (Table 4) can be used as a proxy of the relative size of corresponding loci in a given specimen, at least in such 'opossum-like' metatherians. The m2 is also the widest lower molar in early European peradectids, on average (Gernelle et al. 2024: table 4), and at least in some small early herpetotheriines (Beard and Dawson 2009: fig. 5), but probably not in *Pt. constans* according to the few available measurements (Marandat 1991: table 1).

Because *Pt. maximum* comb. nov. exhibits (i) an M2 with a relatively longer protocone (Table 5; respectively m2 with a probably relatively longer talonid, as the protocone and talonid length must be correlated, see Johanson 1996, p. 1028), and (ii) M2/m2 with a relatively wider protocone/talonid (Table 6; Supplemental material 3: Figures S5-S6) than on M3/m3 on average, unlike *Pt. constans*, and (iii) a protocone of both M2 and M3 relatively longer and (iv) relatively wider than in *Pt. constans* on average (Tables 5-6; respectively m2 and m3 with a talonid on average probably relatively longer and wider in *Pt. maximum* comb. nov.), we suspect that these differences could be explained by a single evolutionary change: the relative enlargement of the protocone – talonid basin complex, more pronounced on the second

molars. Likewise, other subtle, potentially correlated traits related to the enlargement of this functional complex are probably present in *Pt. maximum* comb. nov., as denoted by (i) the high protocone, often higher than instead of as high as or lower than the paracone on several upper molar loci (Figure 3C; pers. obs. KG), (ii) the often relatively large metaconule (e.g., Figure 3B) and (iii) the often relatively mesiodistally long entoconid (e.g., Figure 6A[5]). To our knowledge, *Peratherium maximum* comb. nov. is the single peratheriine exhibiting this combination of characters so far. Such an enlarged protocone – talonid functional complex must also be present in the largest Eocene herpetotheriine, *Herpetotherium comstocki* (Cope, 1884) (see Krishtalka and Stucky 1983a: figs. 1-2). In addition to the recurrence of serial homologs in molars of mammals (Billet and Bardin 2019), even for structures with a less important functional role such as stylar cusps (Crompton and Hiiemae 1970; e.g., all molariform teeth of *Peratherium sudrei* Crochet, 1979, share closely appressed stylar cusps C and D, see Crochet [1980: figs. 168-169]), the existence of the putative correlations described above may reinforce the problem of the 'dearth' of apomorphies, limiting phylogenetic reconstructions in metatherians with an unspecialised tribosphenic dentition (Beck 2023, p. 75).

Relatively larger protocone and talonid basin, as found in *Pt. maximum* comb. nov., must improve crushing capacity and have thus been linked with a more omnivorous diet in metatherians (Wilson 2013, p. 455). The dietary types insectivorous/omnivorous and frugivorous/omnivorous described by Kurz (2007, p. 6) and identified (by comparisons with extant marsupials) in herpetotheriid and in putative peradectid metatherians, respectively (Kurz 2007: table 3), rely only minimally on molar features, thus complicating comparisons with inferences made from isolated molars. For example, the dietary types of the *Peradectes*-like taxon from Messel was inferred close to that of the didelphid *Caluromys* (Kurz 2005), which is mostly frugivorous (e.g., Lessa et al. 2023: fig. 1). Lower molars of *Caluromys* display long and wide talonids with long entoconids (e.g., Flores et al. 2010: fig. 6), and upper molars have the protocones as high as or higher than the paracones (pers. obs. KG). They are similar in these respects to those of *Pt. maximum* comb. nov. Reversely, the European peradectids have relatively short and narrow talonids, as well as relatively low protocones (see illustrations in Gernelle et al. [2024]; note that the latter character probably correlates with faunivory, according to Beck [2015]), contrary to *Caluromys*. This warrants the assessment of the molar morphology of peratheriines and possible peradectid specimens from Messel for further characterisation of Laurasian marsupialiform dietary types. It should be

noted, however, that subtle regional differences in molar shape—investigated using geometric morphometric methods primarily focused on the stylar shelf area and the trigonid—are weakly correlated with differences (if any) in diet in the dentally conservative didelphid marsupials (Chemisquy et al. 2015).

Do the dentally related peculiarities of *Pt. maximum* comb. nov., compared to younger well documented representatives of *Peratherium* and *Amphiperatherium*, justify the erection of a new genus, or at least a distinction between more than one genus in the early Eocene peratheriines, similarly to that initiated by Crochet (1977a) and ancient authors (e.g., Filhol 1879)? It is noteworthy that '*Amphiperatherium*' aff. *maximum* from Geiseltal-Untere Mittelkohle in turn differs from the closely related *Pt. maximum* comb. nov. in its m4 longer than m2 (Storch and Haubold 1989), which does not occur in the latter according to measurements performed on the mandible from La Borie (Table 4) and the mean values of the sample from Condé-en-Brie (Figure 7A-C). Such characters, although important for systematics, are possibly homoplastic and should be reviewed in a phylogenetic context, prior to proposing potential supraspecies groupings for small insectivorous mammals (e.g., Manz and Bloch 2015). The consideration of peratheriine species as part of two early diverging genera, a priori of a study of their evolutionary history via formal phylogenetic analyses, is unlikely, and may lead to misconceptions or incomplete reconstructions of relationships between peratheriine species (e.g., Crochet 1980: figs. 151, 239; Hooker et al. 2008: fig. 5). In other words, if a generic distinction is to be applied between early Eocene peratheriine species, it certainly differs from the deep *Peratherium* – *Amphiperatherium* dichotomy founded by Crochet (1977a, 1977b, 1979, 1980). For these reasons, '*Amphiperatherium*' *maximum* is provisionally and conservatively reallocated to *Peratherium*. Therefore, no species of *Amphiperatherium* have their type locality in the early Eocene of Europe anymore. The occurrences of the typical middle Eocene *A. goethei* and *A. bastbergense* (MP13-MP14), and the late Eocene *A. bourdellense* (MP16-MP17), during the early Eocene (MP8+9-?MP10-11) (Figure 1), as well as their taxonomic status, must be thoroughly tested in other studies.

## Conclusions

A few consistent molar characters, in addition to a size intermediate between those of the most represented metatherian species of the MP7 (*Peratherium constans*) and MP8+9 ('*Amphiperatherium*' *maximum*) reference levels, allowed us to define *Peratherium musivum*,

a new peratheriine species restricted to the MP7-MP8+9 time interval, which was widespread in Western Europe. This revision of MP7-MP8+9 interval molars partly disentangles the complex taxonomy of early peratheriines. We hypothesize close phylogenetic affinities between *Pt. musivum* sp. nov. and *Pt. maximum* comb. nov., the latter being provisionally reallocated to *Peratherium*. A relative enlargement of the protocone/talonid, especially on M2/m2, in *Pt. maximum* comb. nov. is supported by (i) the detailed study of the size and shape of alveoli of a hemi-mandible from La Borie (~MP8+9), the single known for this species; and (ii) our quantitative comparisons of several isolated upper and lower molars. Comparisons between the unique specimen from La Borie and mandibles of among the most representative species of *Peratherium* (*Pt. elegans*) and *Amphiperatherium* (*A. minutum*) revealed more morphological similarities between the latter two species. We established that the previous taxonomic studies focused on Peratheriinae (Crochet 1980; Kurz 2007; Hooker et al. 2008; Ladevèze et al. 2020) did not provide any stable and reliable morphological characters distinguishing *Amphiperatherium* from *Peratherium*, thereby strengthening the conclusions of Ladevèze et al. (2012) regarding the possible non-existence of *Amphiperatherium*, at least in the early Eocene. This study paves the way for further work addressing the taxonomy and intrasubfamilial relationships of the Peratheriinae.


## Acknowledgments

We acknowledge Guillaume Billet (MNHN) for the loan of specimens from the MNHN mammals' collection, under his care. We are also thankful to Vincent N. Pernègre (MNHN), who managed the allocation of various new MNHN specimen numbers (localities of Soissons, Pourcy, Avenay and Condé-en-Brie). Many thanks to the four reviewers, Robin M. D. Beck, Wilma Wessels, Narla S. Stutz and Vicente D. Crespo, for their helpful and constructive comments. This is ISEM publication n° 2024-204.

## Disclosure statement

No potential conflict of interest was reported by the author(s).

## Funding

This research was financially supported by a PhD thesis funding from the French Ministry of Higher Education, Research, and Innovation, and also by the ANR project EDENs [ANR-20-CE02-0007]. Three-dimensional data acquisition was performed using the micro-computed tomography (µ-CT)

facilities of the MRI platform member of the national infrastructure France-BioImaging supported by the French National Research Agency [ANR-10-INBS-04, 'Investments for the future'], the labex CEMEB [ANR-10-LABX-0004] and NUMEV [ANR-10-LABX-0020]. The Leica optical and digital station used to take photographs was acquired as part of the ANR-ERC PALASIAFRICA [ANR-08-JCJC-0017]. 

## ORCID

Killian Gernelle https://orcid.org/0000-0001-9698-0223

Sandrine Ladevèze https://orcid.org/0000-0001- 6009-4107

Rodolphe Tabuce https://orcid.org/0000-0002-4713-3981

## References

Abels HA, Clyde WC, Gingerich PD, Hilgen FJ, Fricke HC, Bowen GJ, Lourens, LJ. 2012. Terrestrial carbon isotope excursions and biotic change during Palaeogene hyperthermals. Nat Geosci. 5:326-329. doi: https://doi.org/10.1038/ngeo1427.

Aymard A. 1850. Compte rendu de la séance du 12 avril 1849, réponse à M. Robert sur les mammifères fossiles des caclcaires du Puy. Ann Soc Agric Sci Puy. 14:80-86.

Beard KC, Dawson MR. 2009. Early Wasatchian mammals of the red hot local fauna, uppermost Tuscahoma Formation, Lauderdale County, Mississippi. Ann Carnegie Mus. 78(3):193–243. doi: https://doi.org/10.2992/007.078.0301.

Beck RMD. 2013. A peculiar faunivorous metatherian from the early Eocene of Australia. Acta Palaeontol Pol. 60(1): 123-129. doi: https://doi.org/10.4202/app.2013.0011.

Beck RMD. 2023. Diversity and phylogeny of marsupials and their stem relatives (Metatheria). In: Cáceres NC, Dickman CR, editors. American and Australasian Marsupials. Cham, Switzerland: Springer; p. 23-88. doi: https://doi.org/10.1007/978-3-031-08419-5_35.

Billet G, Bardin J. 2019. Serial homology and correlated characters in morphological phylogenetics: modeling the evolution of dental crests in placentals. Syst Biol. 68(2):267–280. doi: https://doi.org/10.1093/sysbio/syy071.

BiochroM'97. 1997. Synthèse et tableaux de corrélation. In: Aguilar JP, Legendre S, Michaux J, editors. Actes du Congrès BiochroM'97. Mem Trav EPHE, Inst Montpellier. 21:769-805.

Chemisquy MA, Prevosti FJ, Martin G, Flores DA. 2015. Evolution of molar shape in didelphid marsupials (Marsupialia : Didelphidae): analysis of the influence of ecological factors and phylogenetic legacy. Zool J Linn Soc. 173(1):217-235. doi: https://doi.org/10.1111/zoj.12205.

Clemens WA. 1966. Fossil mammals of the type Lance Formation, Wyoming. Part II, Marsupialia. Univ Calif Publ Geol Sci. 62:1–122.

Costeur L, Schneider M. 2011. Catalogue of the Eocene mammal types of the Natural History Museum Basel. Carnets Geol.

Crespo VD, Goin FJ. 2021. Taxonomy and affinities of african cenozoic metatherians. Span J Palaeont 36(2):1-16. doi: https://doi.org/10.7203/sjp.36.2.20974.

Crespo VD, Goin FJ, Pickford M. 2022. The last African metatherian. Foss Rec. 25(1):173-186. doi: https://doi.org/10.3897/fr.25.80706.

Crochet JY. 1969. Révision du genre *Peratherium* Aymard, 1849 (Marsupialia). C R Acad Sci Paris. 268:2038-2041.

Crochet JY. 1977a. Les Didelphidae (Marsupicarnivora, Marsupialia) holarctiques tertiaires. C R Acad Sci Paris. 284:357-360.

Crochet JY. 1977b. Les didelphidés paléogènes holarctiques : historique et tendances évolutives. Geobios Mem spec. 1:127–134.

Crochet JY. 1978. La poche à phosphate de Ste-Néboule (Lot) et sa faune de vertébrés du Ludien supérieur. 7- Didelphides (Marsupiaux). Palaeovertebrata. 8(2-4):231-242.

Crochet JY. 1979. Diversité systématique des Didelphidae (Marsupialia) européens tertiaires. Geobios. 12(3):365–378.

Crochet JY. 1980. Les marsupiaux du Tertiaire d'Europe. Paris: Edtions Foundation Singer-Polignac.

Crochet JY. 2016. Valbro: A new site of vertebrates from the early Oligocene (MP 22) of France (Quercy). IV – Marsupialia, Insectivora. Ann Paleontol. 102(1):7-10. doi: https://doi.org/10.1016/j.annpal.2015.12.001.

Crompton AW, Hiiemae K. 1970. Molar occlusion and mandibular movements during occlusion in the American opossum, *Didelphis marsupialis* L. Zool J Linn Soc. 49(1):21-47. doi: https://doi.org/10.1111/j.1096-3642.1970.tb00728.x.

Dégremont E, Duchaussois F, Hautefeuille F, Laurain M, Louis P, Tétu R. 1985. Paléontologie: découverte d'un gisement du Cuisien tardif à Prémontré (Aisne). Bull Inf Géol Bass Paris. 22(2): 11-18.

Delacre M, Christophe L, Mora YL, Lakens D. 2019. Taking parametric assumptions seriously: arguments for the use of Welch's *F*-test instead of the classical *F*-test in one-way ANOVA. Int Rev Soc Psychol. 32(1):13. doi: https://doi.org/10.5334/irsp.198.

Depéret C, Douxami H. 1902. Les vertébrés Oligocènes de Pyrimont-Challonges (Savoie). Mem Soc Pal Suisse. 29:1–90.

Dunn RH, Townsend KEB. 2019. New pantolestids from the Uinta Formation, Utah. J Vertebr Paleontol. e1652622. doi: https://doi.org/10.1080/02724634.2019.1652622.

Estravís C. 2000. Nuevos mamíferos del Eoceno Inferior de Silveirinha (Baixo Mondego, Portugal). Coloquios Paleontol. 51:281–311.

Filhol H. 1877. Recherches sur les Phosphorites du Quercy. Étude des fossiles qu'on y rencontre et

spécialement des Mammifères. Ann Sci Geol. 8:1-340.

Filhol H. 1879. Étude des Mammifères fossiles de Saint-Gérand-le-Puy. Ann Sci Geol. 10:1-253.

Filhol H. 1881. Étude des Mammifères fossiles de Ronzon (Haute-Loire). Ann Sci Geol. 12:1-270.

Flores DA, Abdala F, Giannini N. 2010. Cranial ontogeny of *Caluromys philander* (Didelphidae: Caluromyinae): a qualitative and quantitative approach. J Mammal. 91(3):539-550. doi: https://doi.org/10.1644/09-MAMM-A-291.1.

Flynn LJ, Barry JC, Morgan ME, Pilbeam D, Jacobs LL, Lindsay E.H. 1995. Neogene Siwalik mammalian lineages: species longevities, rates of change, and modes of speciation. Palaeogeogr Palaeoclimatol Palaeoecol. 115(1-4):249-264. doi: https://doi.org/10.1016/0031-0182(94)00114-N.

Gazin CL. 1952. The lower Eocene Knight Formation of western Wyoming and its mammalian faunas. Smithson Misc Collect. 117(18):1-82.

Gernelle K, Billet G, Gheerbrant E, Godinot M, Marandat B, Ladevèze S, Tabuce R. 2024. Taxonomy and evolutionary history of peradectids (Metatheria): new data from the early Eocene of France. J Mamm Evol. 31(3):31. doi: https://doi.org/10.1007/s10914-024-09724-5.

Godinot M. 1981. Les mammifères de Rians (Eocène inférieur, Provence). Palaeovertebrata. 10(2):43–126.

Godinot M, Crochet JY, Hartenberger JL, Lange-Badré B, Russell DE, Sigé B. 1987. Nouvelles données sur les mammifères de Palette (Eocène inférieur, Provence). Münch Geowiss Abh (A). 10:273-288.

Gordon CL. 2003. A first look at estimating body size in dentally conservative marsupials. J Mamm Evol. 10(1-2):1-21. doi: https://doi.org/10.1023/A:1025545023221.

Hand SJ, Sigé B, Archer M, Gunnell GF, Simmons NB. 2015. A new early Eocene (Ypresian) bat from Pourcy, Paris Basin, France, with comments on patterns of diversity in the earliest chiropterans. J Mamm Evol. 22:343–354. doi: https://doi.org/10.1007/s10914-015-9286-9.

Hoek Ostende LW van den, Bilgin M, Braumuller Y, Cailleux F, Skandalos P. 2023. Live long and prosper? Assessing longevity of small mammal taxa using the NOW database. In: Casanovas-Vilar I, Hoek Ostende LW van den, Janis CM, Saarinen J, editors. Evolution of Cenozoic Land Mammal Faunas and Ecosystems: 25 Years of the NOW Database of Fossil Mammals, Vertebrate Paleobiology and Paleoanthropology. Cham, Switzerland: Springer; p. 111–129. doi: https://doi.org/10.1007/978-3-031-17491-9_8.

Hooker JJ. 1996a. Mammalian biostratigraphy across the Paleocene-Eocene boundary in the Paris, London and Belgian basins. In: Knox RWOB, Corfield RM, Dunay RE, editors. Correlation of the Early Paleogene in Northwest Europe. Geol Soc Lond, Spec Publ. 101:205–218. doi: https://doi.org/10.1144/gsl.sp.1996.101.01.13.

Hooker JJ. 1996b. Mammals from the Early (late Ypresian) to Middle (Lutetian) Eocene Bracklesham Group, southern England. Tert Res. 16(1-4):141-174.

Hooker JJ. 1998. Mammalian faunal change across the Paleocene-Eocene transition in Europe. In: Aubry MP, Lucas SG, Berggren WA, editors. Late Paleocene-Early Eocene Climatic and Biotic Events in the Marine and Terrestrial Records. New York: Columbia University Press; p. 428-450.

Hooker JJ. 2010. The mammal fauna of the early Eocene Blackheath formation of Abbey Wood, London. Monogr Palaeontogr Soc. 164(634):1–153. doi: https://doi.org/10.1080/25761900.2022.12131814.

Hooker JJ, Cook E, Benton MJ. 2005. British Tertiary fossil mammal GCR sites. In: Benton MJ, Cook E, JJ Hooker, editors. Mesozoic and Tertiary Fossil Mammals and Birds of Great Britain. Geol Conserv Rev Ser. 32:67-124. Peterborough: Joint Nature Conservation Committee.

Hooker JJ, Sánchez-Villagra MR, Goin FJ, Simons EL, Attia Y, Seiffert ER. 2008. The origin of Afro-Arabian 'didelphimorph' marsupials. Palaeontology. 51(3):635-648. doi: https://doi.org/10.1111/j.1475-4983.2008.00779.x.

Horovitz I, Ladevèze S, Argot C, Macrini TE, Martin T, Hooker JJ, Kurz C, Muizon C de, Sánchez-Villagra MR. 2008. The anatomy of *Herpetotherium* cf. *fugax* Cope, 1873, a metatherian from the Oligocene of North America. Palaeontogr Abt A. 284(4-6):109–141. doi: https://doi.org/10.1127/pala/284/2008/109.

International Commission of Zoological Nomenclature (ICZN). 1999. International Code of Zoological Nomenclature. London: The International Trust for Zoological Nomenclature. http://www.nhm.ac.uk/hosted-sites/iczn/code/

Johanson Z. 1996. New marsupial from the Fort Union Formation, Swain Quarry, Wyoming. J Paleontol. 70(6):1023–1031.

Koenigswald W von. 1970. *Peratherium* (Marsupialia) im Ober-Oligozän und Miozän von Europa. Bayer Akad Wiss Math-Natur Kl Abh (NF). 144:1–79.

Korth WW. 1994. Middle Tertiary marsupials (Mammalia) from North America. J Paleontol. 68(2):376–397.

Korth WW. 2008 Marsupialia. In: Janis CM, Gunnell GF, Uhen MD, editors. Evolution of Tertiary Mammals of North America: Volume 2, Small Mammals, Xenarthrans, and Marine Mammals. Cambridge: Cambridge University Press; p. 39-47.

Krishtalka L, Stucky RK. 1983a. Revision of the Wind River faunas, early Eocene of Central Wyoming. Part 3. Marsupialia. Ann Carnegie Mus. 52(9):205–227.

Krishtalka L, Stucky RK. 1983b. Paleocene and Eocene marsupials of North America. Ann Carnegie Mus. 52(10):229–263.

Kurz C. 2005. Ecomorphology of opossum-like marsupials from the Tertiary of Europe and a comparison with selected taxa. Kaupia. 14:21–26.

Kurz C. 2007. The opossum-like marsupials (Didelphimorphia and Peradectia, Marsupialia, Mammalia) from the Eocene of Messel and Geiseltal – Ecomorphology, diversity and palaeogeography. Kaupia. 15:3–65.

Kurz C, Habersetzer J. 2004. Untersuchungen der zahnmorphologie von beutelratten aus Messel mit der mikroröntgenmethode CORR. Cour Forsch-Inst Senckenberg. 252:13–21.

Ladevèze S, Muizon C de, Beck RMD, Germain D, Cespedes-Paz R. 2011. Earliest evidence of mammalian social behaviour in the basal Tertiary of Bolivia. Nature. 474:83–86. doi: https://doi.org/10.1038/nature09987.

Ladevèze S, Selva C, Muizon C de. 2020. What are "opossum-like" fossils? The phylogeny of

herpetotheriid and peradectid metatherians, based on new features from the petrosal anatomy. J Syst Palaeontol. 18(17):1463–1479. doi: https://doi.org/10.1080/14772019.2020.1772387.

Ladevèze S, Smith R, Smith T. 2012. Reassessment of the morphology and taxonomic status of the earliest herpetotheriid marsupials of Europe. J Mamm Evol. 19:249–261. doi: https://doi.org/10.1007/s10914-012-9195-0.

Laurent Y, Adnet S, Bourdon E, Corbalan D, Danilo L, Duffaud S, Fleury G, Garcia G, Godinot M, Le Roux G, et al. 2010. La Borie (Saint-Papoul, Aude): un gisement exceptionnel dans l'Éocène basal du Sud de la France. Bull Soc Hist Nat Toulouse. 146:89-103.

Lebrun R, Orliac MJ. 2016. MorphoMuseuM: an online platform for publication and storage of virtual specimens. Paleontol Soc Pap. 22:183-195. doi: https://doi.org/10.1017/scs.2017.14.

Legendre S, Marandat B, Sigé B, Crochet JY, Godinot M, Hartenberger JL, Sudre J, Vianey-Liaud M, Muratet B, Astruc JG. 1992. La faune de mammifères de Vielase (phosphorites du Quercy, Sud de la France): Preuve paléontologique d'une karstification du Quercy dès l'Eocène inférieur. Neues Jahrb Geol Paläontol. 7:414–428.

Lösel PD, Kamp T van de, Jayme A, Ershov A, Faragó T, Pichler O, Tan Jerome N, Aadepu N, Bremer S, Chilingaryan SA, et al. 2020. Introducing Biomedisa as an open-source online platform for biomedical image segmentation. Nat Commun. 11:5577. doi: https://doi.org/10.1038/s41467-020-19303-w.

Louis P. 1966. Note sur un nouveau gisement situé à Condé-en-Brie (Aisne) et renfermant des restes de mammifères de l'Eocène inférieur. Ann Univ A.R.E.R.S. Reims. 4:108–118.

Louis P. 1996. Recherches de mammifères paléogènes dans les départements de l'Aisne et de la Marne pendant la deuxième moitié du vingtième siècle. Palaeovertebrata. 25(2-4):83–113.

Louis P, Laurain M. 1983. Nouveau gisement de vertébrés dans le Cuisien supérieur de Saint-Agnan (Aisne). Ses relations stratigraphiques avec les autres gisements yprésiens du Bassin parisien. Bull Inf Géol Bass Paris. 20(4):3–20.

Louis P, Michaux J. 1962. Présence de mammifères sparnaciens dans les sablières de Pourcy (Marne). C R Somm Seances Soc Geol Fr. 6:170–171.

Luccisano V, Sudre J, Lihoreau F. 2020. Revision of the Eocene artiodactyls (Mammalia, Placentalia) from Aumelas and Saint-Martin-de-Londres (Montpellier limestones, Hérault, France) questions the early European artiodactyl radiation. J Syst Palaeontol. 18(19):1631-1656. doi: https://doi.org/10.1080/14772019.2020.1799253.

Manz CL, Bloch JI. 2015 Systematics and phylogeny of Paleocene-Eocene Nyctitheriidae (Mammalia, Eulipotyphla?) with description of a new species from the late Paleocene of the Clarks Fork Basin, Wyoming, USA. J Mamm Evol. 22:307–342. doi: https://doi.org/10.1007/s10914-014-9284-3.

Marandat B. 1986. Decouverte d'une faune de micromammiferes d'âge cuisien superieur dans les marno-calcaires d'Agel à Azillanet (Minervois, Hérault). Geol Fr. 2:197–204.

Marandat B. 1991. Mammifères de l'Ilerdien Moyen (Eocène Inférieur) des Corbières et du Minervois. Palaeovertebrata. 20(2-3):55–144.

Marandat B, Adnet S, Marivaux L, Martinez A, Vianey-Liaud M, Tabuce R. 2012. A new mammalian

fauna from the earliest Eocene (Ilerdian) of the Corbières (Southern France): Palaeobiogeographical implications. Swiss J Geosci. 105:417–434. doi: https://doi.org/10.1007/s00015-012-0113-5.

Marivaux L, Vianey-Liaud M, Jaeger JJ. 2004. High-level phylogeny of early Tertiary rodents: dental evidence. Zool J Linn Soc. 142:105-134. doi: https://doi.org/10.1111/j.1096-3642.2004.00131.x.

Marshall CR. 2017. Five palaeobiological laws needed to understand the evolution of the living biota. Nat Ecol Evol. 1:165. doi: https://doi.org/10.1038/s41559-017-0165.

Martin GM. 2005. Intraspecific variation in *Lestodelphys halli* (Marsupialia: Didelphimorphia). J Mammal. 86(4):793–802. doi: https://doi.org/10.1644/1545-1542(2005)086[0793:IVILHM]2.0.CO;2.

Martin JE, Case JA, Jagt JWM, Schulp AS, Mulder EWA. 2005. A new European marsupial indicates a Late Cretaceous high-latitude transatlantic dispersal route. J Mamm Evol. 12(3-4):495–511. doi: https://doi.org/10.1007/s10914-005-7330-x.

McGrew PO, Berman JE, Hecht MK, Hummel JM, Simpson GG, Wood AE. 1959. The geology and paleontology of the Elk Mountain and Tabernacle Butte area, Wyoming. Bull Am Mus Nat Hist. 117(3):121-176.

Muizon C de, Ladevèze S. 2022. New material of *Incadelphys antiquus* (Pucadelphyda, Metatheria, Mammalia) from the early Palaeocene of Bolivia reveals phylogenetic affinities with enigmatic North and South American metatherians. Geodiversitas. 44(22):609–643. doi: https://doi.org/10.5252/geodiversitas2022v44a22.

Murphey PC, Kelly TS, Chamberlain KR, Tsukui K, Clyde WC. 2018. Mammals from the earliest Uintan (middle Eocene) Turtle Bluff Member, Bridger Formation, southwestern Wyoming, USA, Part 3: Marsupialia and a reevaluation of the Bridgerian-Uintan North American Land Mammal Age transition. Palaeontol Electron. 21(2):25A: 1–52. https://doi.org/10.26879/804.

Nel A, de Plöeg G, Dejax J, Dutheil D, de Franceschi D, Gheerbrant E, Godinot M, Hervet S, Menier JJ, Augé M, et al. 1999. Un gisement sparnacien exceptionnel à plantes, arthropodes et vertébrés (Eocène basal, MP7): Le Quesnoy (Oise, France). C R Acad Sci Paris. 329:65–72. doi: https://doi.org/10.1016/S1251-8050(99)80229-8.

Noiret C, Steurbaut E, Tabuce R, Marandat B, Schnyder J, Storme JY, Yans J. 2016. New bio-chemostratigraphic dating of a unique early sequence from southern Europe results in precise mammalian biochronological tie-points. Newsl Stratigr. 49(3):469–480. doi: https://doi.org/10.1127/nos/2016/0336.

Peláez-Campomanes P, Peña A de la, López Martínez N. 1989. Primeras faunas de micromamíferos del Paleógeno de La Cuenca del Duero. Stud Geol Salmant, Vol Esp. 5:135-157.

Peters GJY. 2017. userfriendlyscience: Quantitative analysis made accessible. R package version 0.7.2. doi: https://doi.org/10.17605/osf.io/txequ.

Philip J, Vianey-Liaud M, Martin-Closas C, Tabuce R, Léonide P, Margerel JP, Noël J. 2017. Stratigraphy of the Haut Var Paleogene continental series (Northeastern Provence, France): New insight on the age of the 'Sables bleutés du Haut Var' Formation. Geobios. 50(4):319–339. doi: https://doi.org/10.1016/j.geobios.2017.06.002

Prieto J., Rummel M. 2015. On a well-preserved mandible of *Amphiperatherium* from the Middle

Miocene fissure filling Petersbuch 39: one of the youngest record of Metatheria (Mammalia) in Germany. Zitteliana A. 55:121–126.

R Core Team. 2024. R: A language and environment for statistical computing. Vienna, Austria: R Foundation for Statistical Computing.

Rémy JA, Aguilar JP, Crochet JY, Duffaud S, Escarguel G, Godinot M, Marandat B, Michaux J, Rage JC, Sigé B, et al. 1997. Les remplissages karstiques polyphasés (Eocène, Oligocène, Miocène), de Saint‐Maximin (Phosphorites du Gard) et leur apport à la connaissance des faunes européennes, notamment pour l'Eocène moyen (MPI3). 1. Introduction, systématique (pars) et synthèse. In: Aguilar JP, Legendre S, Michaux J, editors. Actes du Congrès BiochroM'97. Mém Trav EPHE, Inst Montpellier. 21:711-728.

Russell DE, Galoyer A, Louis P, Gingerich PD. 1988. Nouveaux vertébrés sparnaciens du Conglomérat de Meudon à Meudon, France. C R Acad Sci Paris. 307:429–433.

Ruxton GD, Beauchamp G. 2008. Time for some a priori thinking about post hoc testing. Behav Ecol. 19(3):690-693. doi: https://doi.org/10.1093/beheco/arn020.

Sánchez-Villagra M, Ladevèze S, Horovitz I, Argot C, Hooker JJ, Macrini TE, Martin T, Moore-Fay S, Muizon C de, Schmelzle T, Asher RJ. 2007. Exceptionally preserved North American Paleogene metatherians: Adaptations and discovery of a major gap in the opossum fossil record. Biol Lett. 3(3):318–322. doi: https://doi.org/10.1098/rsbl.2007.0090.

Selva C, Ladevèze S. 2017. Computed microtomography investigation of the skull of Cuvier's famous 'opossum' (Marsupialiformes, Herpetotheriidae) from the Eocene of Montmartre. Zool J Linn Soc. 180(3):672-693. doi: https://doi.org/10.1111/zoj.12495.

Simons EL, Bown TM. 1984. A new species of *Peratherium* (Didelphidae; Polyprotodonta): the first African marsupial. J Mammal. 65(4):539-548. doi: https://doi.org/10.2307/1380836.

Simpson GG. 1930. Post-Mesozoic Marsupialia. In: Pompeckj JF, editor. Fossilium Catalogus. I: Animalia. Pars 47. Berlin: W. Junk; p. 1-87.

Smith R., Russell DE. 1992. Mammifères (Marsupialia, Chiroptera) de l'Yprésien de la Belgique. Bull Inst Royal Sci Nat Belgique, Sci Terre. 62:223-227.

Smith R, Smith T. 2004. Les mammifères de l'Yprésien moyen du Bassin de Paris (niveau-repère MP8-9) sont-ils présents dès la limite Paléocène-Eocène de Dormaal (niveau-repère MP7, Belgique)? Oryctos. 5:75-82.

Solé F, Falconnet J, Laurent Y. 2014. New proviverrines (Hyaenodontida) from the early Eocene of Europe; phylogeny and ecological evolution of the Proviverrinae. Zool J Linn Soc. 171(4):878-917. doi: https://doi.org/10.1111/zoj.12155.

Solé F, Godinot M, Laurent Y, Galoyer A, Smith T. 2018. The European mesonychid mammals: Phylogeny, ecology, biogeography, and biochronology. J Mamm Evol. 25:339–379. doi: https://doi.org/10.1007/s10914-016-9371-8.

Speijer RP, Pälike H, Hollis CJ, Hooker JJ, Ogg JG. 2020. The Paleogene Period. In: Gradstein FM, Ogg JG, Schmitz MD, Ogg GM, editors. Geologic Time Scale 2020. Amsterdam: Elsevier; p. 1087–1140. doi: https://doi.org/10.1016/B978-0-12-824360-2.00028-0.

Spijkerman E, van Nieulande FAD, Wesselingh FP, Reich S, Tracey S. 2015. Pourcy (Paris Basin, France): preliminary assessment of an early Eocene NW European tropical coastal environment

from molluscs and vertebrate fossils. Cainozoic Res. 15(1-2):155–180.

Steurbaut E, Magioncalda R, Dupuis C, van Simaeys S, Roche E, Roche M. 2003. Palynology, paleoenvironments, and organic carbon isotope evolution in lagoonal Paleocene-Eocene boundary settings in North Belgium. Spec Pap Geol Soc Am. 369:291–317.

Storch G. 1993. *Amphiperatherium goethei*, ein weiteres Beuteltier aus dem Eozän von Messel (Mammalia, Didelphidae). Carolinea. 51:123-124.

Storch G, Haubold H. 1989. Additions of the Geiseltal mammalian faunas, Middle Eocene: Didelphidae, Nyctitheriidae, Myrmecophagidae. Palaeovertebrata. 19(3):95-114.

Sudre J, Sigé B, Rémy JA, Marandat B, Hartenberger JL, Godinot M, Crochet JY. 1990. Une faune du niveau d'Egerkingen (MP 14; Bartonien inférieur) dans les phosphorites du Quercy (Sud de la France). Palaeovertebrata. 20(1):1-32.

Szalay FS. 1993. Metatherian taxon phylogeny: Evidence and interpretation from the cranioskeletal system. In: Szalay FS, Novacek MJ, McKenna MC, editors. Mammal Phylogeny, Vol. 1. Mesozoic Differentiation, Multituberculates, Monotremes, Early Therians, and Marsupials. New York: Springer-Verlag; p. 216-242.

Tarquini SD, Ladevèze S, Prevosti FJ. 2022. The multicausal twilight of South American native mammalian predators (Metatheria, Sparassodonta). Sci Rep. 12:1224. doi: https://doi.org/10.1038/s41598-022-05266-z.

Vianey-Liaud M, Lihoreau F, Solé F, Gernelle K, Vautrin Q, Bronnert C, Bourget H, Vidalenc D, Tabuce R. 2024. A revision of the late early Eocene mammal faunas from Mas de Gimel and Naples (Montpellier, Southern France) and the description of a new theridomorph rodent. Geodiversitas. 46(10):387-422. doi: https://doi.org/10.5252/geodiversitas2024v46a7.

Wessels W, Weerd AA van de, Marković Z. 2024. Marsupials (herpetotheriids) from the late Palaeogene of south-east Serbia. Palaeobio Palaeoenv. doi: https://doi.org/10.1007/s12549-024-00600-x.

Wickham H. 2016. ggplot2: Elegant graphics for data analysis. Use R!, Springer. doi: https://doi.org/10.1007/978-3-319-24277-4.

Williamson TE, Brusatte SL, Carr TD, Weil A, Standhardt BR. 2012. The phylogeny and evolution of Cretaceous-Palaeogene metatherians: Cladistic analysis and description of new early Palaeocene specimens from the Nacimiento Formation, New Mexico. J Syst Palaeontol. 10(4):625–651. doi: https://doi.org/10.1080/14772019.2011.631592.

Wilson GP. 2013. Mammals across the K/Pg boundary in northeastern Montana, U.S.A.: dental morphology and body-size patterns reveal extinction selectivity and immigrant-fueled ecospace filling. Paleobiology. 39(3):429-469. doi: https://doi.org/10.1666/12041.

Yans J, Marandat B, Masure E, Serra-Kiel J, Schnyder J, Storme JY, Marivaux L, Adnet S, Vianey-Liaud M, Tabuce R. 2014. Refined bio-(benthic foraminifera, dinoflagellate cysts) and hemostratigraphy (δ13Corg) of the earliest Eocene at Albas-Le Clot (Corbières, France): Implications for mammalian biochronology in Southern Europe. Newsl Stratigr. 47(3):331–353. doi: https://doi.org/10.1127/nos/2014/0050.

**Supplemental material 1.** Ratio values of stylar shelf to talon length, stylar shelf to protocone length, talon to protocone length, and talon to protocone width (see Figure 2 for measurement protocols) of each M2 and M3 specimen sampled for *Peratherium constans*, *Pt. musivum* sp. nov., and *Pt. maximum* comb. nov. The holotype specimens and associated values are depicted in bold text.

| Locus | Species | Specimen | sL/tL | sL/pL | tL/pL | tW/pW |
|---|---|---|---|---|---|---|
| M2 | *Pt. constans* | **IRSNB-M-1** | **1.81** | **2.90** | **1.59** | **-** |
| | | IRSNB-M-2 | 1.78 | 2.87 | 1.62 | 2.52 |
| | | IRSNB-M-1324 | 1.69 | 2.39 | 1.41 | 1.92 |
| | | IRSNB-M-2039 | 1.79 | 2.42 | 1.35 | 1.94 |
| | | IRSNB-M-2040 | 1.69 | 2.15 | 1.28 | 2.05 |
| | | NBM Om.1 | 1.85 | 2.69 | 1.45 | 2.04 |
| | | NBM Om.158 | 1.61 | 2.23 | 1.39 | 2.08 |
| | | NBM Om.159 | 1.62 | 2.51 | 1.55 | 2.46 |
| | *Pt. musivum* sp. nov. | MNHN.F.Ri220 | - | - | 1.33 | 1.85 |
| | *Pt. maximum* comb. nov. | MNHN.F.CB5116 | 1.70 | 2.25 | 1.32 | 1.77 |
| | | MNHN.F.CB196 | 1.71 | 2.13 | 1.25 | 1.92 |
| | | MNHN.F.CB197 | 1.64 | 1.94 | 1.18 | 1.61 |
| | | MNHN.F.CB5119 | 1.60 | 2.01 | 1.26 | 1.67 |
| | | MNHN.F.CB5112 | 1.68 | 2.12 | 1.26 | 1.62 |
| | | MNHN.F.CB5121 | 1.67 | 2.10 | 1.26 | 1.92 |
| | | MNHN.F.CB1327 | 1.61 | 1.85 | 1.15 | 1.59 |
| | | MNHN.F.CB3322 | 1.61 | 2.02 | 1.25 | 1.65 |
| | | MNHN.F.CB4128 | 1.53 | 1.83 | 1.19 | 1.59 |
| M3 | *Pt. constans* | IRSNB-M-1331 | 1.68 | 2.32 | 1.38 | 2.00 |
| | | IRSNB-M-1332 | 1.52 | 2.35 | 1.54 | 2.34 |
| | | IRSNB-M-1333 | 1.49 | 2.26 | 1.52 | 1.88 |
| | | IRSNB-M-2030 | 1.59 | 2.62 | 1.65 | 2.53 |
| | | IRSNB-M-2041 | 1.50 | 2.34 | 1.56 | 2.21 |
| | | IRSNB-M-2042 | 1.72 | 2.79 | 1.63 | 2.58 |
| | | UM-FDN-10 | 1.67 | 2.42 | 1.45 | 2.00 |
| | *Pt. musivum* sp. nov. | **MNHN.F.SN122** | **1.64** | **2.21** | **1.35** | **1.69** |
| | | MNHN.F.SN14 | 1.60 | 2.13 | 1.34 | 1.84 |
| | *Pt. maximum* comb. nov. | MNHN.F.CB5115 | 1.75 | 2.87 | 1.64 | 2.28 |
| | | MNHN.F.CB5117 | 1.63 | 2.06 | 1.27 | 1.63 |
| | | MNHN.F.CB195 | 1.56 | 1.97 | 1.26 | - |
| | | **MNHN.F.CB198** | **1.70** | **2.35** | **1.38** | **1.79** |
| | | MNHN.F.CB5118 | 1.64 | 2.40 | 1.46 | 1.99 |
| | | MNHN.F.CB1252 | 1.56 | 2.00 | 1.28 | 1.88 |
| | | MNHN.F.CB1397 | 1.65 | 2.18 | 1.32 | 1.95 |
| | | MNHN.F.CB4121 | 1.69 | 2.29 | 1.35 | 1.77 |
| | | MNHN.F.CB4142 | 1.59 | 2.17 | 1.36 | 1.77 |

**Supplemental material 2.** Length (L), width (W), trigonid width (trW) and talonid width (tlW) measurements (in mm) of all isolated m1 to m4 of *Peratherium maximum* comb. nov. from the type locality, Condé-en-Brie (~MP8+9). Length to width ratios (L/W) are calculated for each specimen.

| Specimen | Locus | L | W | L/W | trW | tlW | tlWr |
|---|---|---|---|---|---|---|---|
| MNHN.F.CB5088 | m1 | 2,57 | 1,55 | 1,66 | 1,26 | 1,52 | 0,43 |
| MNHN.F.CB207 | m1 | 2,6 | 1,47 | 1,77 | 1,21 | 1,44 | 0,42 |
| MNHN.F.CB5101 | m1 | 2,49 | 1,5 | 1,66 | 1,23 | 1,45 | 0,43 |
| MNHN.F.CB577 | m1 | 2,58 | 1,57 | 1,64 | 1,36 | 1,53 | 0,41 |
| MNHN.F.CB5120 | m1 | 2,56 | 1,59 | 1,61 | 1,32 | 1,54 | 0,42 |
| MNHN.F.CB807 | m1 | 2,38 | 1,46 | 1,63 | 1,21 | 1,42 | 0,45 |
| MNHN.F.CB841 | m1 | 2,6 | 1,47 | 1,77 | 1,18 | 1,42 | 0,42 |
| MNHN.F.CB854 | m1 | 2,44 | 1,59 | 1,53 | 1,31 | 1,57 | 0,45 |
| MNHN.F.CB1179 | m1 | 2,47 | 1,49 | 1,66 | 1,21 | 1,42 | 0,44 |
| MNHN.F.CB5125 | m1 | 2,54 | 1,5 | 1,69 | 1,27 | 1,44 | 0,42 |
| MNHN.F.CB2709 | m1 | 2,59 | 1,57 | 1,65 | 1,26 | 1,5 | 0,42 |
| MNHN.F.CB2715 | m1 | 2,47 | 1,46 | 1,69 | 1,19 | 1,42 | 0,44 |
| MNHN.F.CB2812 | m1 | 2,47 | 1,5 | 1,65 | 1,23 | 1,46 | 0,44 |
| MNHN.F.CB2896 | m1 | 2,7 | 1,6 | 1,69 | 1,32 | 1,57 | 0,40 |
| MNHN.F.CB2933 | m1 | 2,6 | 1,58 | 1,65 | 1,27 | 1,54 | 0,42 |
| MNHN.F.CB3305 | m1 | 2,58 | 1,54 | 1,68 | 1,29 | 1,52 | 0,42 |
| MNHN.F.CB3336 | m1 | 2,38 | 1,43 | 1,66 | 1,19 | 1,38 | 0,45 |
| MNHN.F.CB3398 | m1 | 2,32 | 1,5 | 1,55 | 1,16 | 1,44 | 0,48 |
| MNHN.F.CB4118 | m1 | 2,49 | 1,58 | 1,58 | 1,3 | 1,56 | 0,44 |
| MNHN.F.CB5105 | m2 | 2,62 | 1,6 | 1,64 | 1,45 | 1,6 | 0,40 |
| MNHN.F.CB593 | m2 | 2,85 | 1,73 | 1,65 | 1,57 | 1,71 | 0,37 |
| MNHN.F.CB608 | m2 | 2,73 | 1,69 | 1,62 | 1,52 | 1,64 | 0,38 |
| MNHN.F.CB648 | m2 | 2,61 | 1,58 | 1,65 | 1,44 | 1,52 | 0,39 |
| MNHN.F.CB781 | m2 | 2,57 | 1,67 | 1,54 | 1,47 | 1,61 | 0,41 |
| MNHN.F.CB826 | m2 | 2,65 | 1,66 | 1,60 | 1,54 | 1,6 | 0,38 |
| MNHN.F.CB829 | m2 | 2,8 | 1,87 | 1,50 | 1,6 | 1,79 | 0,38 |
| MNHN.F.CB831 | m2 | 2,79 | 1,71 | 1,63 | 1,55 | 1,71 | 0,38 |
| MNHN.F.CB832 | m2 | 2,63 | 1,7 | 1,55 | 1,46 | 1,7 | 0,41 |
| MNHN.F.CB838 | m2 | 2,51 | 1,65 | 1,52 | 1,38 | 1,62 | 0,43 |
| MNHN.F.CB839 | m2 | 2,7 | 1,77 | 1,53 | 1,55 | 1,76 | 0,39 |
| MNHN.F.CB5122 | m2 | 2,78 | 1,75 | 1,59 | 1,55 | 1,7 | 0,38 |
| MNHN.F.CB5123 | m2 | 2,65 | 1,67 | 1,59 | 1,45 | 1,62 | 0,40 |
| MNHN.F.CB5124 | m2 | 2,67 | 1,59 | 1,68 | 1,43 | 1,52 | 0,39 |

| | | | | | | | |
|---|---|---|---|---|---|---|---|
| MNHN.F.CB3421 | m2 | 2,71 | 1,76 | 1,54 | 1,53 | 1,75 | 0,39 |
| MNHN.F.CB3635 | m2 | 2,78 | 1,65 | 1,68 | 1,52 | 1,62 | 0,37 |
| MNHN.F.CB4125 | m2 | 2,75 | 1,75 | 1,57 | 1,55 | 1,69 | 0,38 |
| MNHN.F.CB4666 | m2 | 2,67 | 1,64 | 1,63 | 1,43 | 1,64 | 0,40 |
| MNHN.F.CB4707 | m2 | 2,61 | 1,7 | 1,54 | 1,48 | 1,68 | 0,41 |
| MNHN.F.CB208 | m3 | 2,74 | 1,68 | 1,63 | 1,62 | 1,68 | 0,37 |
| MNHN.F.CB5109 | m3 | 2,6 | 1,6 | 1,63 | 1,49 | 1,51 | 0,39 |
| MNHN.F.CB5110 | m3 | 2,61 | 1,59 | 1,64 | 1,49 | 1,55 | 0,39 |
| MNHN.F.CB698 | m3 | 2,71 | 1,57 | 1,73 | 1,56 | 1,5 | 0,36 |
| MNHN.F.CB746 | m3 | 2,73 | 1,72 | 1,59 | 1,59 | 1,58 | 0,37 |
| MNHN.F.CB821 | m3 | 2,72 | 1,65 | 1,65 | 1,57 | 1,63 | 0,37 |
| MNHN.F.CB836 | m3 | 2,65 | 1,56 | 1,70 | 1,52 | 1,51 | 0,38 |
| MNHN.F.CB1115 | m3 | 2,62 | 1,6 | 1,64 | 1,47 | 1,52 | 0,39 |
| MNHN.F.CB1116 | m3 | 2,63 | 1,57 | 1,68 | 1,52 | 1,56 | 0,39 |
| MNHN.F.CB2802 | m3 | 2,69 | 1,7 | 1,58 | 1,61 | 1,67 | 0,38 |
| MNHN.F.CB3295 | m3 | 2,68 | 1,58 | 1,70 | 1,57 | 1,58 | 0,37 |
| MNHN.F.CB3433 | m3 | 2,7 | 1,58 | 1,71 | 1,49 | 1,52 | 0,37 |
| MNHN.F.CB4127 | m3 | 2,81 | 1,68 | 1,67 | 1,6 | 1,63 | 0,36 |
| MNHN.F.CB4977 | m3 | 2,63 | 1,57 | 1,68 | 1,52 | 1,55 | 0,38 |
| MNHN.F.CB655 | m4 | 2,43 | 1,37 | 1,77 | 1,36 | 1,26 | 0,40 |
| MNHN.F.CB820 | m4 | 2,38 | 1,25 | 1,90 | 1,25 | 1,18 | 0,41 |
| MNHN.F.CB825 | m4 | 2,54 | 1,39 | 1,83 | 1,39 | 1,3 | 0,38 |
| MNHN.F.CB855 | m4 | 2,53 | 1,36 | 1,86 | 1,36 | 1,17 | 0,37 |
| MNHN.F.CB1316 | m4 | 2,72 | 1,45 | 1,88 | 1,45 | 1,23 | 0,34 |
| MNHN.F.CB4126 | m4 | 2,53 | 1,43 | 1,77 | 1,36 | 1,23 | 0,38 |
| MNHN.F.CB4170 | m4 | 2,5 | 1,43 | 1,75 | 1,43 | 1,16 | 0,36 |
| MNHN.F.CB4178 | m4 | 2,49 | 1,36 | 1,83 | 1,36 | 1,09 | 0,36 |

**Supplemental material 3** Results of Games-Howell post hoc tests (GH) performed on isolated m1-m4 of *Peratherium maximum* comb. nov. from Condé-en-Brie (~MP8+9), and boxplots of the absolute and relative labiolingual width of the talonid compared between loci. Statistical differences are recovered between pairs of lower molar loci when $p < 0.05$.

Figure S1. GH result for the mesiodistal length (L).

| | diff | ci.lo | ci.hi | t | df | p |
|---|---|---|---|---|---|---|
| m2-m1 | 0.17 | 0.09 | 0.25 | 5.73 | 35.82 | <.001 |
| m3-m1 | 0.16 | 0.09 | 0.24 | 6.00 | 30.41 | <.001 |
| m4-m1 | 0.00 | -0.12 | 0.12 | 0.06 | 12.69 | 1.000 |
| m3-m2 | -0.01 | -0.08 | 0.06 | 0.33 | 30.83 | .988 |
| m4-m2 | -0.17 | -0.29 | -0.05 | 4.26 | 11.94 | .005 |
| m4-m3 | -0.17 | -0.28 | -0.05 | 4.27 | 9.98 | .008 |

Figure S2. GH result for the labiolingual width (W).

| | diff | ci.lo | ci.hi | t | df | p |
|---|---|---|---|---|---|---|
| m2-m1 | 0.17 | 0.11 | 0.22 | 8.21 | 33.57 | <.001 |
| m3-m1 | 0.09 | 0.04 | 0.15 | 4.86 | 27.60 | <.001 |
| m4-m1 | -0.14 | -0.22 | -0.07 | 5.64 | 11.55 | .001 |
| m3-m2 | -0.07 | -0.13 | -0.01 | 3.34 | 30.83 | .011 |
| m4-m2 | -0.31 | -0.39 | -0.23 | 11.29 | 14.83 | <.001 |
| m4-m3 | -0.24 | -0.32 | -0.16 | 8.87 | 13.24 | <.001 |

Figure S3. GH result for labiolingual width of the talonid (tlW).

| | diff | ci.lo | ci.hi | t | df | p |
|---|---|---|---|---|---|---|
| m2-m1 | 0.18 | 0.12 | 0.24 | 8.00 | 34.66 | <.001 |
| m3-m1 | 0.09 | 0.03 | 0.15 | 4.20 | 28.25 | .001 |
| m4-m1 | -0.28 | -0.36 | -0.20 | 10.27 | 12.30 | <.001 |
| m3-m2 | -0.09 | -0.15 | -0.02 | 3.67 | 30.62 | .005 |
| m4-m2 | -0.45 | -0.54 | -0.37 | 15.76 | 14.82 | <.001 |
| m4-m3 | -0.37 | -0.45 | -0.29 | 12.99 | 13.66 | <.001 |

Figure S4. GH result for estimated surface area (S = L/2 * trW + L/2 * tlW), where S is the surface area; L is the mesiodistal length, trW is the trigonid width, and tlW is the talonid width.

| | diff | ci.lo | ci.hi | t | df | p |
|---|---|---|---|---|---|---|
| m2-m1 | 0.80 | 0.57 | 1.03 | 9.46 | 34.90 | <.001 |
| m3-m1 | 0.73 | 0.52 | 0.95 | 9.19 | 29.36 | <.001 |
| m4-m1 | -0.20 | -0.49 | 0.08 | 2.11 | 13.83 | .199 |
| m3-m2 | -0.07 | -0.31 | 0.17 | 0.79 | 30.91 | .860 |
| m4-m2 | -1.01 | -1.30 | -0.71 | 9.77 | 16.54 | <.001 |
| m4-m3 | -0.94 | -1.23 | -0.65 | 9.47 | 14.29 | <.001 |

Figure S5. GH result for the labiolingual width of the trigonid relative to approximate surface (tlWr) calculated as: tlWR = tlW / S, where tlW is the labiolingual talonid width, and S is the estimated surface area.

| | diff | ci.lo | ci.hi | t | df | p |
|---|---|---|---|---|---|---|
| m2-m1 | -0.04 | -0.05 | -0.03 | 7.22 | 35.18 | <.001 |
| m3-m1 | -0.06 | -0.07 | -0.04 | 10.80 | 29.81 | <.001 |
| m4-m1 | -0.06 | -0.08 | -0.03 | 6.25 | 11.06 | <.001 |
| m3-m2 | -0.02 | -0.03 | 0.00 | 3.28 | 30.90 | .013 |
| m4-m2 | -0.02 | -0.04 | 0.01 | 1.89 | 9.96 | .293 |
| m4-m3 | 0.00 | -0.03 | 0.03 | 0.17 | 8.86 | .998 |

Figure S6. Boxplots of the absolute (A) (tlW, in mm; see Figure S3) and relative (B) labiolingual width of the talonid (tlWr; see Figure S5) of all isolated m1s to m4s of *Peratherium maximum* comb. nov. from Condé-en-Brie (~MP8+9).